FUSELAGE-MOUNTED ANTENNA CODE - User's Manual

W. D. Burnside
R. J. Marhefka
E. L. Pelton

D D C

13 MAR 1979

E

Department of the Navy
Naval Air Development Center
Warminster, Pennsylvania 18974

79 03 12 150

SECURITY CLASSIFICATION OF THIS PAGE *(When Data Entered)*

REPORT DOCUMENTATION PAGE		READ INSTRUCTIONS BEFORE COMPLETING FORM
1. REPORT NUMBER NADC-79042-30	2. GOVT ACCESSION NO.	3. RECIPIENT'S CATALOG NUMBER
4. TITLE *(and Subtitle)* FUSELAGE-MOUNTED ANTENNA CODE - User's Manual		5. TYPE OF REPORT & PERIOD COVERED Technical Report
		6. PERFORMING ORG. REPORT NUMBER ESL 4583-2 (784583)
7. AUTHOR(s) W. D. Burnside R. J. Marhefka E. L. Pelton		8. CONTRACT OR GRANT NUMBER(s) Contract N62269-76-C-0554
9. PERFORMING ORGANIZATION NAME AND ADDRESS The Ohio State University ElectroScience Laboratory, Department of Electrical Engineering Columbus, Ohio 43212		10. PROGRAM ELEMENT, PROJECT, TASK AREA & WORK UNIT NUMBERS 63206N,WR6-1154 WTW180000,RA702
11. CONTROLLING OFFICE NAME AND ADDRESS Department of the Navy Naval Air Development Center Warminster, Pennsylvania 18974		12. REPORT DATE July 1977
		13. NUMBER OF PAGES 72
14. MONITORING AGENCY NAME & ADDRESS*(if different from Controlling Office)*		15. SECURITY CLASS. *(of this report)* Unclassified
		15a. DECLASSIFICATION/DOWNGRADING SCHEDULE

16. DISTRIBUTION STATEMENT *(of this Report)*

Approved for public release; distribution unlimited

17. DISTRIBUTION STATEMENT *(of the abstract entered in Block 20, if different from Report)*

18. SUPPLEMENTARY NOTES

19. KEY WORDS *(Continue on reverse side if necessary and identify by block number)*

Airborne antennas	Computer code manual
Calculated volumetric patterns	Input/output data description
High frequency solutions	
Geometrical theory of diffraction	

20. ABSTRACT *(Continue on reverse side if necessary and identify by block number)*

This manual describes the input and output data associated with the volumetric computer code which has been delivered to the Naval Air Development Center. The input data is defined in general terms and applied to the Boeing 737 aircraft. Numerous examples are included to illustrate the various features of the computer code.

DD _{1 JAN 73} FORM 1473   EDITION OF 1 NOV 65 IS OBSOLETE

SECURITY CLASSIFICATION OF THIS PAGE *(When Data Entered)*

TABLE OF CONTENTS

I. INTRODUCTION

For the past several years, the ElectroScience Laboratory (ESL) has been very successful in developing numerical solutions via the Geometrical Theory of Diffraction (GTD) approach for the radiation patterns of antennas mounted on aircraft [1-7]. These numerical solutions provide a useful, efficient, and economical way for the evaluation, location, and design of fuselage-mounted antennas based on their pattern performance in the principal planes. However, if modern systems are to function properly, the antenna pattern must meet certain specifications. These specifications are usually given in terms of a coverage diagram for a particular sector in space for the antenna mounted on the aircraft not on a finite ground plane where the original antenna design was made. Thus, the desire for an accurate solution for the complete pattern performance of antennas mounted on a complex aircraft structure for given applications requires a more thorough study of ways to handle the volumetric pattern.

First, it has been shown by numerous scale model measurements that our roll plane model can be extended to almost cover the complete volumetric pattern except for two conical sectors (fore and aft) [3]. The limitations of the roll plane model result are due to the finite length fuselage. Yet, the finite length fuselage has been solved, previously, in our elevation plane model analyses. Furthermore, based on our previous three-dimensional studies of geodesic rays which contribute to the pattern of an antenna on various spheroids, one is able to combine the analyses of these two principal planes to give the complete volumetric pattern [6,7]. In addition, the cockpit/radome section and stabilizers are taken into account using the flat or bent plate model previously used to analyze the wings in the roll plane. Using this approach, the complete volumetric pattern is obtained using a model consisting of a composite elliptic cylinder to which are attached flat or bent plates. As a result of this simplified model, the program is very efficient and requires little computer storage space. This numerical solution also provides both amplitude and phase data.

This report describes briefly the way our elevation and roll plane model solutions are combined to give the complete volumetric pattern for fuselage-mounted airborne antennas. For more details on this solution refer to Reference [7]. The aircraft simulation model used in the analysis is discussed in Section II. A complete description of the input data and organization of the main program is presented in Section III. A sample simulation of the 737 aircraft is considered in Section IV. Various examples which illustrate the versatility of the code are presented in Section V. Finally, a numerical technique is developed in Appendix A which can be used to simplify the simulation of the fuselage.

1

II. COMPUTER MODEL OF AN AIRCRAFT

In our study, computer simulation models are considered that resemble a wide variety of aircraft shapes and yet can, also, be analyzed with reasonable accuracy and economy. In this case, the three-dimensional nature of the fuselage must be modeled if one is to adequately determine volumetric patterns. This requirement resulted in the development of a general surface of revolution model of the aircraft fuselage as presented in Reference [2]. Through an extensive study of geodesic paths on a general surface of revolution, the number of dominant rays that contribute to the radiation pattern was shown to be finite except for a sphere. Furthermore, the numerical result showed that, for a prolate spheroid, the dominant rays needed to be considered would not exceed four; in most cases, it is even less than that. These four rays are illustrated in Figure 1 in which two rays are propagating around the
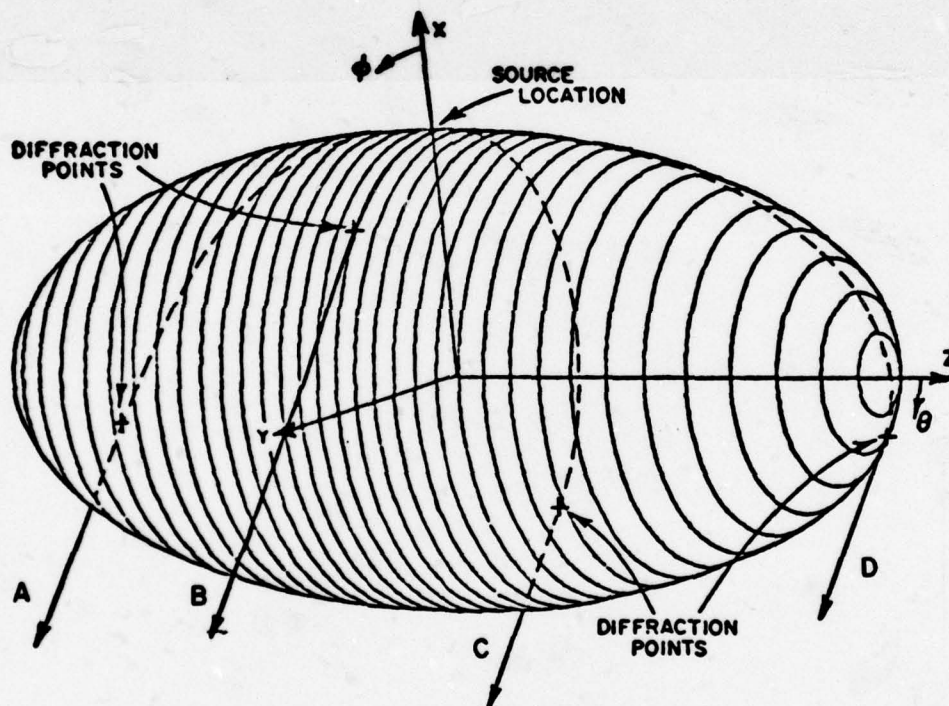
Figure 1. The four dominant GTD terms that radiate at $\theta = 90°$, $\phi = 145°$.

cross-section of the prolate spheroid; the other two are propagating along the profile. To demonstrate the significance of these four rays, the elevation plane pattern of an axial slot mounted on a prolate spheroid was calculated using a two-dimensional (two rays) and three-dimensional (four rays)

2

solution as shown in Figure 2. Experimental results were also shown to verify the calculated three-dimensional result. It is immediately obvious from those results that the back lobe region is not predicted using the two-dimensional result. The two-dimensional result being the principal plane pattern of a slot on an elliptic cylinder where the elliptic cross-section simulates the profile of the prolate spheroid. This model only considers the two rays which propagate along the profile (i.e., rays A and D in Figure 1). However, the three-dimensional solution for the prolate spheroid [2] is in good agreement with the measured pattern. The prolate spheroid solution requires excessive computer time and storage and for those reasons the present approach to handle the three-dimensional fuselage was developed.

As determined previously, our roll plane model of the aircraft (refer to Figure 6a) was capable of successfully computing the volumetric pattern except for the fore and aft sectors illustrated in Figure 3. However, these two sectors were accurately treated using our elevation plane model of the aircraft (refer to Figure 6b). Consequently, a method was developed which combines these two solutions to give the complete pattern. Recall that four rays contribute to the radiation pattern in the shadow region for an antenna mounted on a prolate spheroid. Since there are only two significant rays which propagate around an electrically large elliptic cylinder, both the elevation and roll plane cylinders are needed to calculate the four ray effect. In order to blend these two cylinder solutions together, a belt region is used as illustrated in Figure 4. Within this region the elevation plane model applies in that it provides the dominant two rays. Outside the belt region the roll plane model is used in that it provides the dominant rays. The angle α is chosen such that the roll and elevation solutions blend smoothly together. In fact, α is a function of the size of elevation and roll plane cylinders used to simulate the aircraft fuselage. For most cases in our model, the angle α is set at 20°. This 20° belt has been tested and found to be satisfactory, based on comparisons with measured results.

Using this new efficient solution, the elevation pattern of an axial slot mounted on a prolate spheroid was calculated using the input data given in Section V and is illustrated in Figure 5. The comparison between the measured and calculated results is very persuasive. This is a very effective test for the solution in that the spheroid is small and nearly spherical as opposed to the large and more cylindrical fuselage shape. The curvature of the fuselage in the vicinity of the antenna location plays a dominant role in predicting the radiation pattern. Thus, the elliptic cylinders which are used to represent the fuselage profile and cross-section should model the aircraft structure as accurately as possible near the antenna location. In order to simulate the aircraft shape at the antenna location a best fit ellipse routine is included in Appendix A. This routine can be used to generate the roll (or cross-section) ellipse and elevation (or profile) composite ellipse.
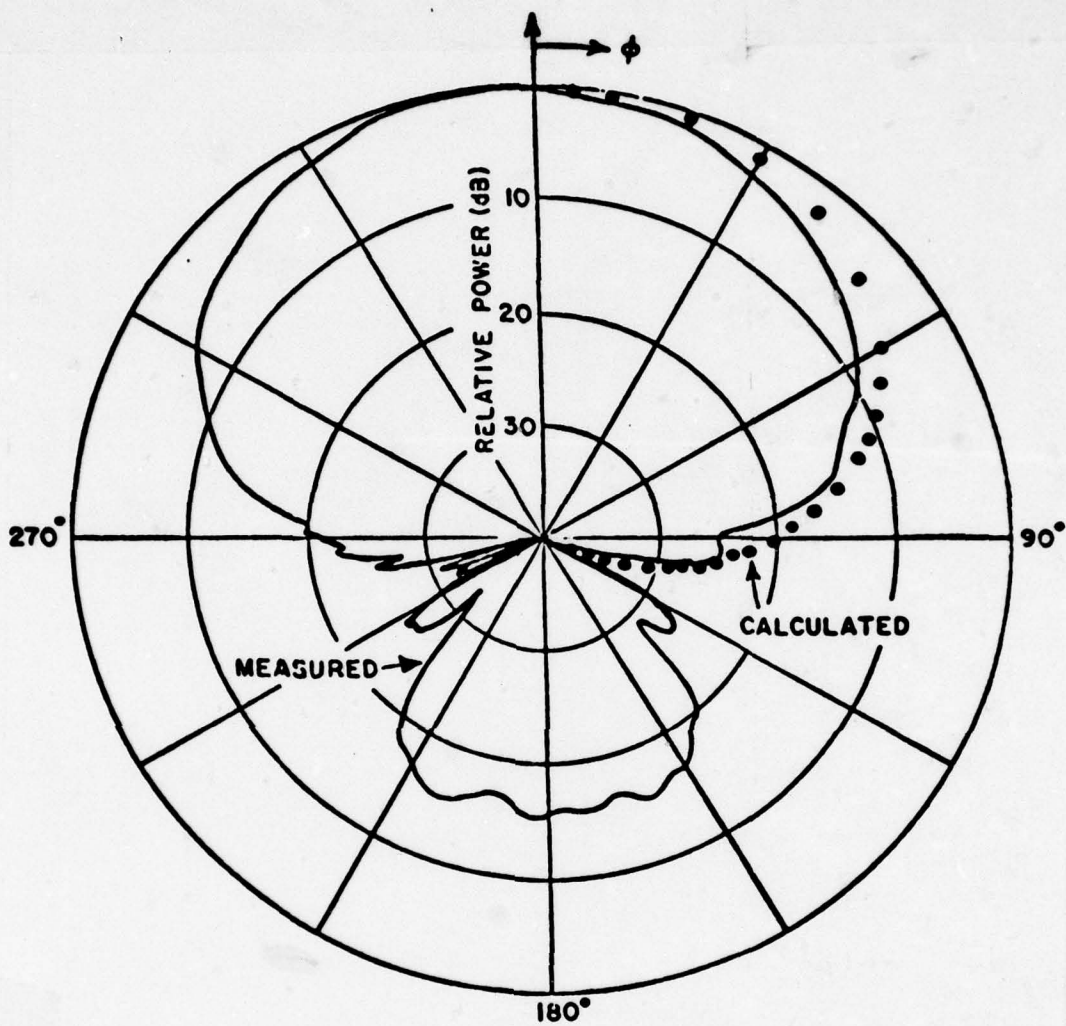
3

Figure 2(a). Elevation plane pattern of an axial slot mounted on a 4λ x 2λ prolate spheroid with the two-dimensional theoretical solution presented.

4

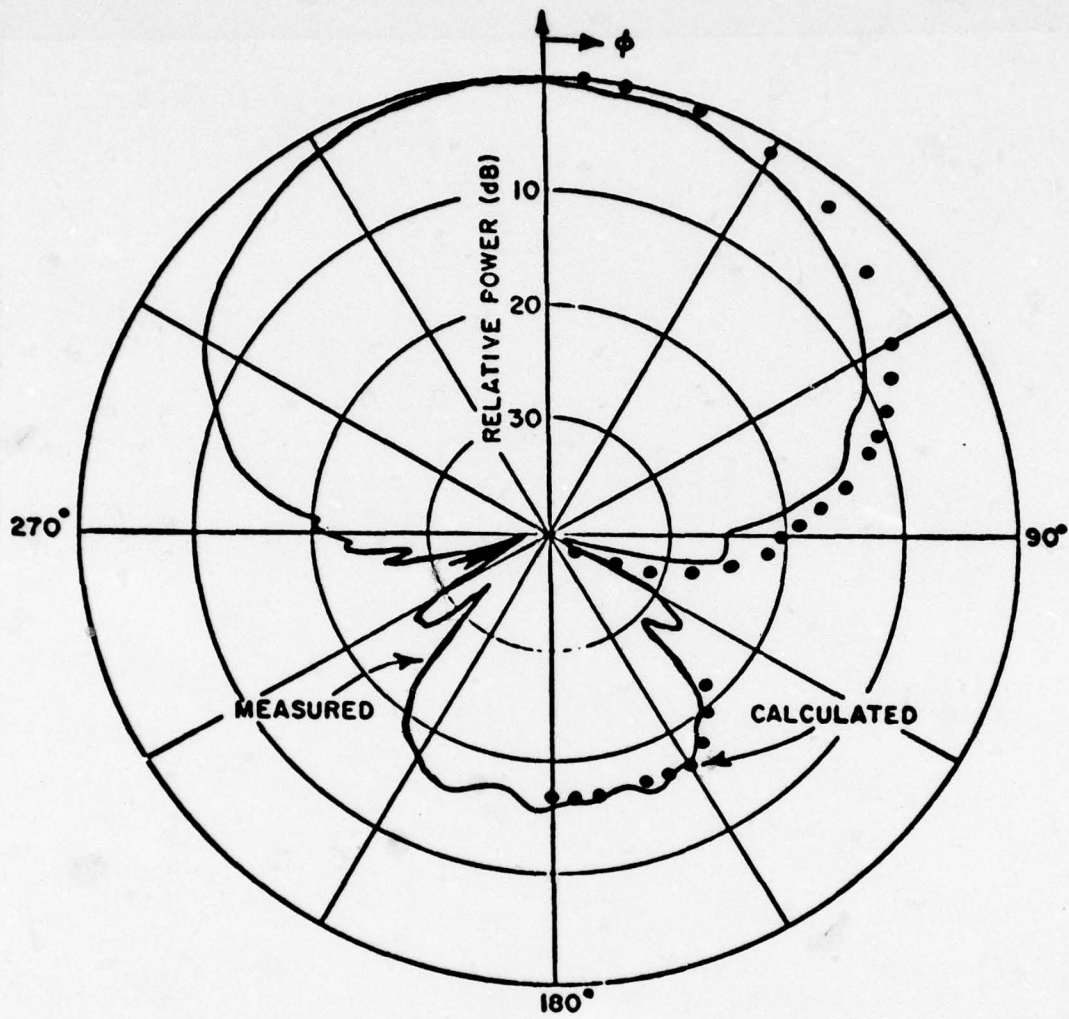Figure 2(b). Elevation plane pattern of an axial slot mounted on a 4λ x 2λ prolate spheroid with the three-dimensional theoretical solution presented.

5

15° CONICAL
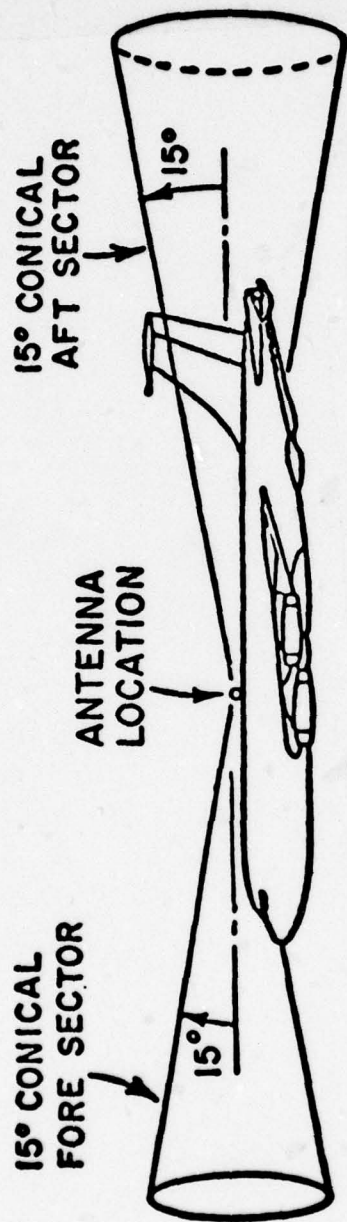AFT SECTOR

15°

ANTENNA
LOCATION

15° CONICAL
FORE SECTOR

15°

Figure 3. Fore and aft sectors outside of which our "Roll Plane Model" is valid.

6
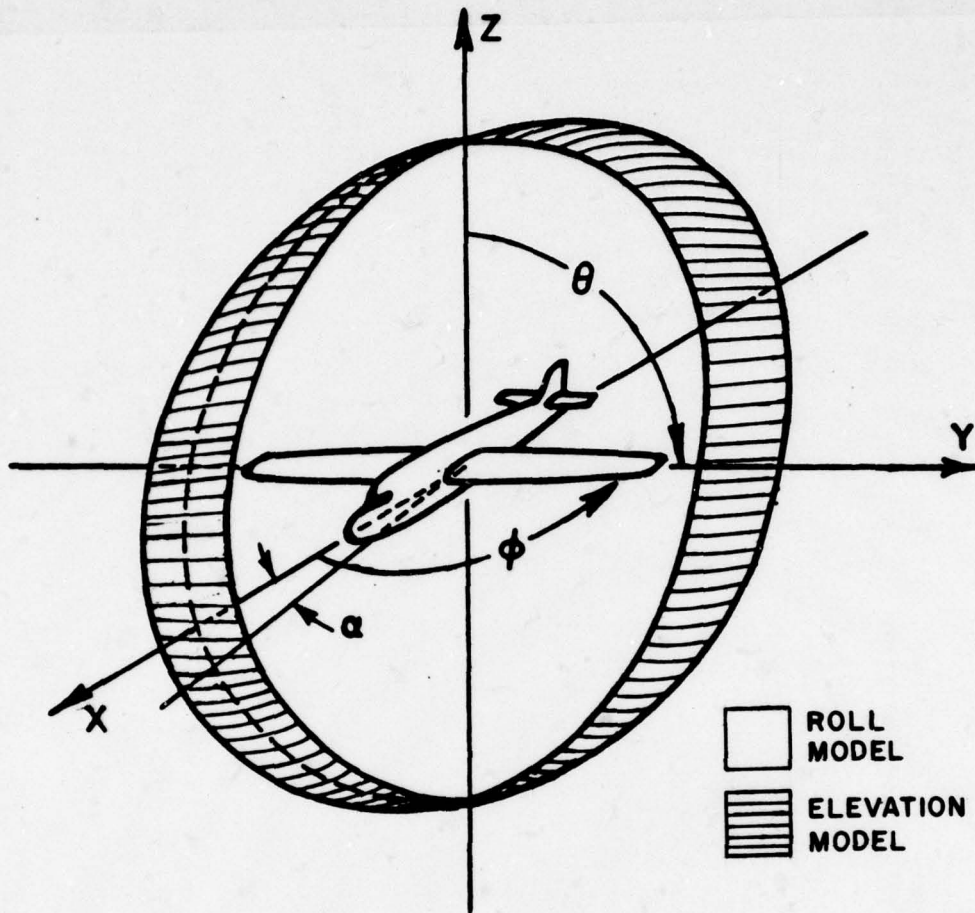
Figure 4. Illustration of belt region in which elevation
plane model analysis is employed.
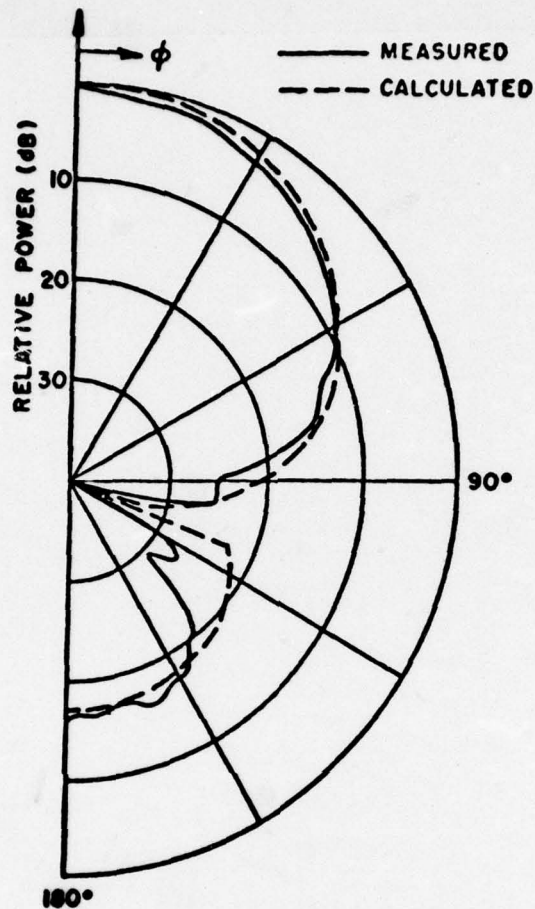
Figure 5. Elevation plane pattern of an axial slot mounted on a 4λ x 2λ prolate spheroid using newly developed volumetric solution. (Geometry illustrated in Figure 1.)

With the roll and elevation plane cylinders defined, one attaches flat or bent plates to them to simulate the wings and horizontal stabilizers in the roll model and nose section and vertical stabilizer in the elevation model. These models are illustrated in Figure 6. Note that there is a separate coordinate system used for the two models. The elevation model coordinates are defined by the subscript "e" or "elev"; whereas, the roll model coordiates use "r" or "roll". The connection between the two coordinate systems is depicted in Figure 7.

8
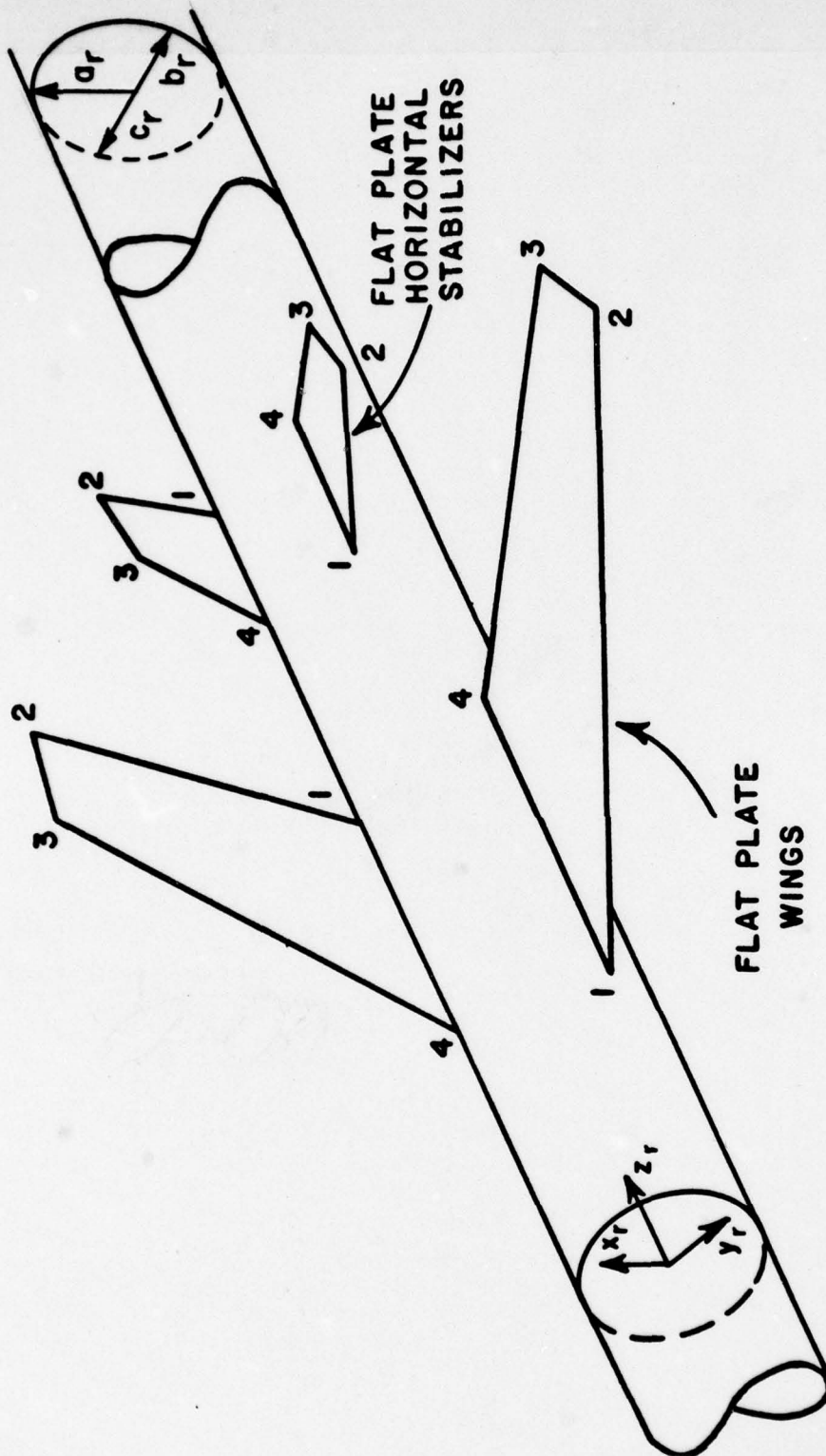
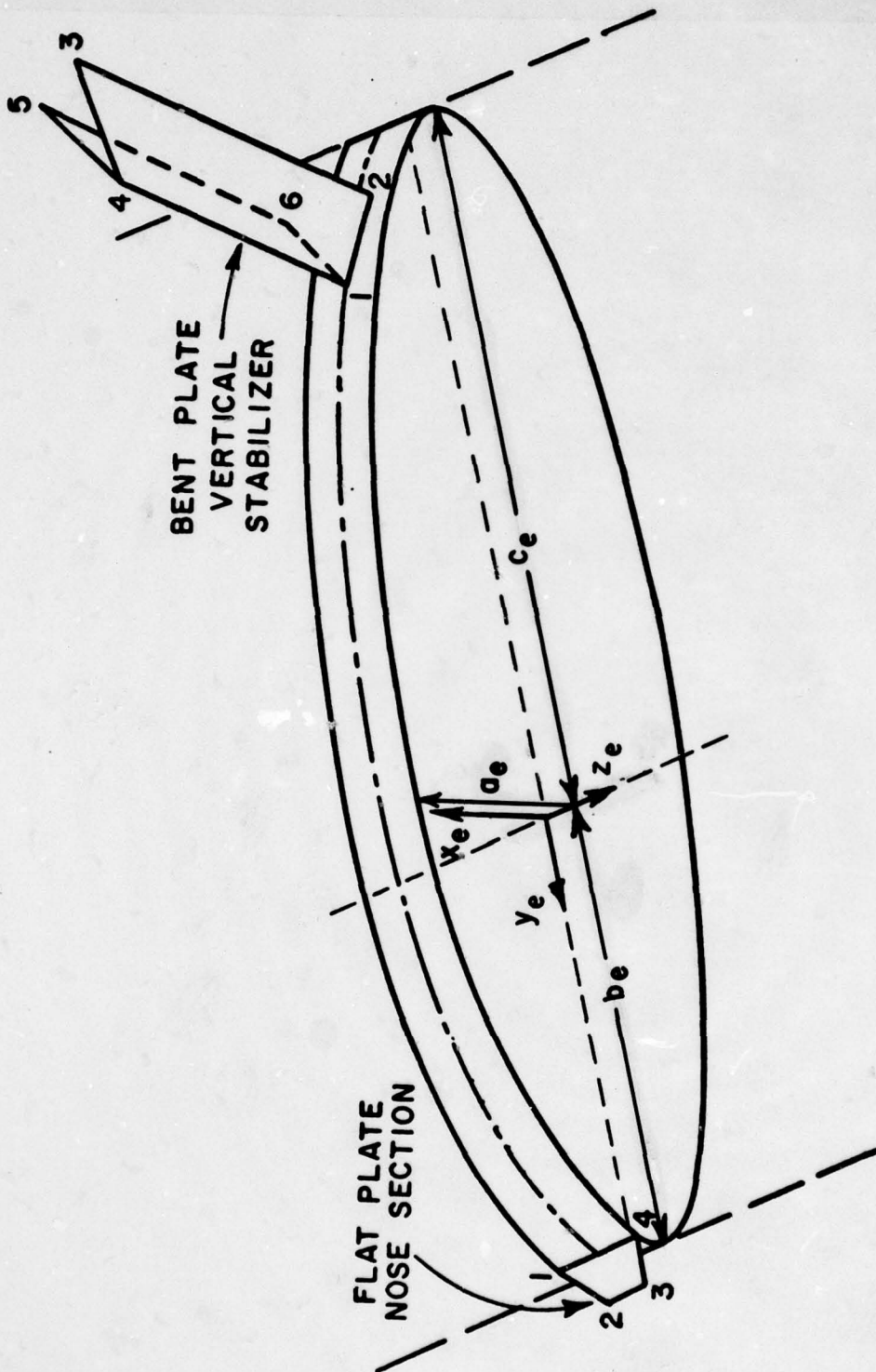Figure 6(a). Illustration of roll plane model.

9

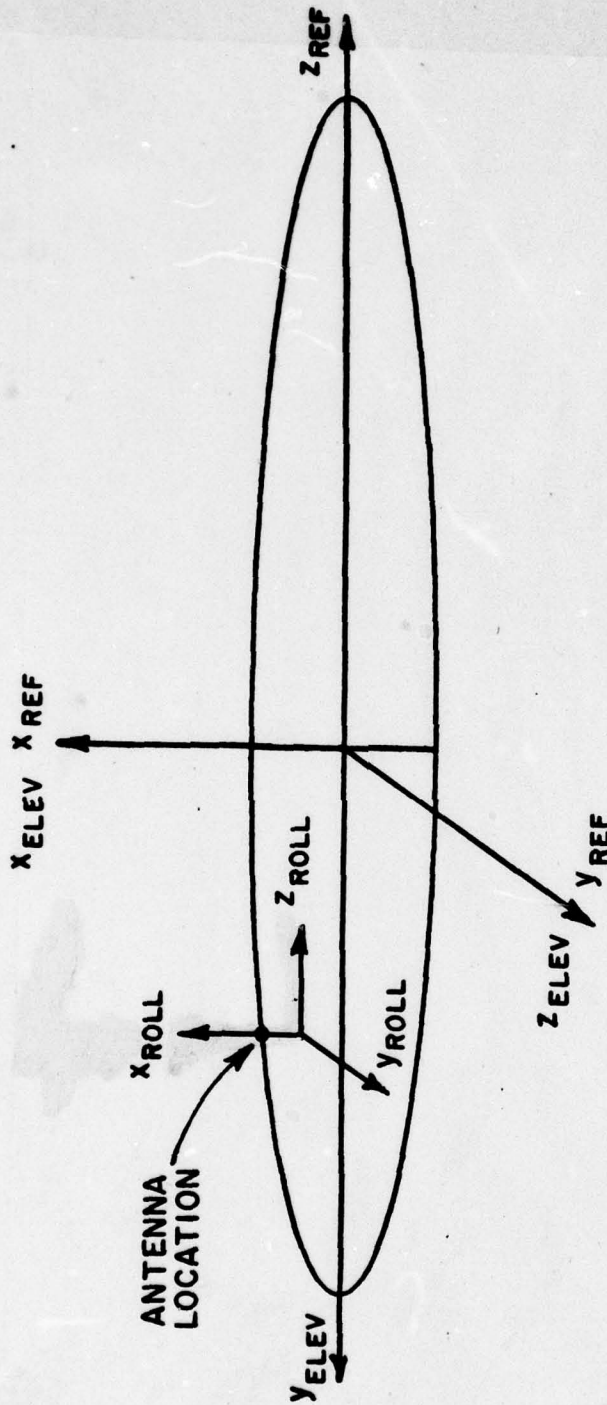Figure 6(b). Illustration of elevation plane model.

Figure 7. Illustration of various coordinate systems used in our volumetric pattern analysis for center-line mounted antennas.

11

The flat or bent plates used to simulate the aircraft wings and stabilizers are described by defining the location of the plate corners in terms of appropriate Cartesian coordinate system (XYZ_{roll} or XYZ_{elev} system) as shown in Figure 6. The corners are numbered in a counter clockwise sense with the first corner being on the cylinder. The plate can be horizontally mounted up and down on the cylinder as illustrated in Figure 8. However, when the plates are mounted on the lower half elliptic cylinder (X_r or X_e is negative), the y component of the first and last corners are set equal to the semi major or minor axis of the ellipse as seen in Figure 8. This modification is made to eliminate the interior wedge problem which leads to multiple reflections and diffractions. Since the antenna is restricted to be on the top or near the top of the cylinder, this modification is reasonable. In addition, the field contribution from this edge is small compared with the other edges of the plate. This is due to the great attenuation of the surface wave propagating along the cylinder surface in reaching the edge. Note that the plates are not restricted to lie horizontally. They can be tilted forward, backward, or sideways as seen in Figure 9. However for the forward or backward tilting, the plates are required to lie below the y axis with x negative. This requirement is necessary because the wedge angle (the angle between the cylinder and plate) must be constant for a given edge.

In general, flat plates in the roll plane model are used to model the aircraft wings. However for some aircraft such as the F-4, bent plates are necessary to simulate the bent wings. Bent plates can, also, be used to simulate the wing flaps.

The scale model drawings of the aircraft are used to determine the coordinates of the corners of the plates which simulate the nose section, wings and stabilizers. The X_r and Y_r coordinates of the corners which specify wings or horizontal stabilizers are measured from the front view of the aircraft. The Z_r component is determined from the top view of the scale model drawing. Similarly, the X_e and Y_e coordinates of the corners specifying the vertical stabilizer and nose section are measured from the side view of the aircraft. The Z_e component is obtained from the top view of the aircraft. Note that if the antenna is mounted on the bottom of the fuselage, then the aircraft should be flipped over so that the antenna appears to be mounted on top of the aircraft.
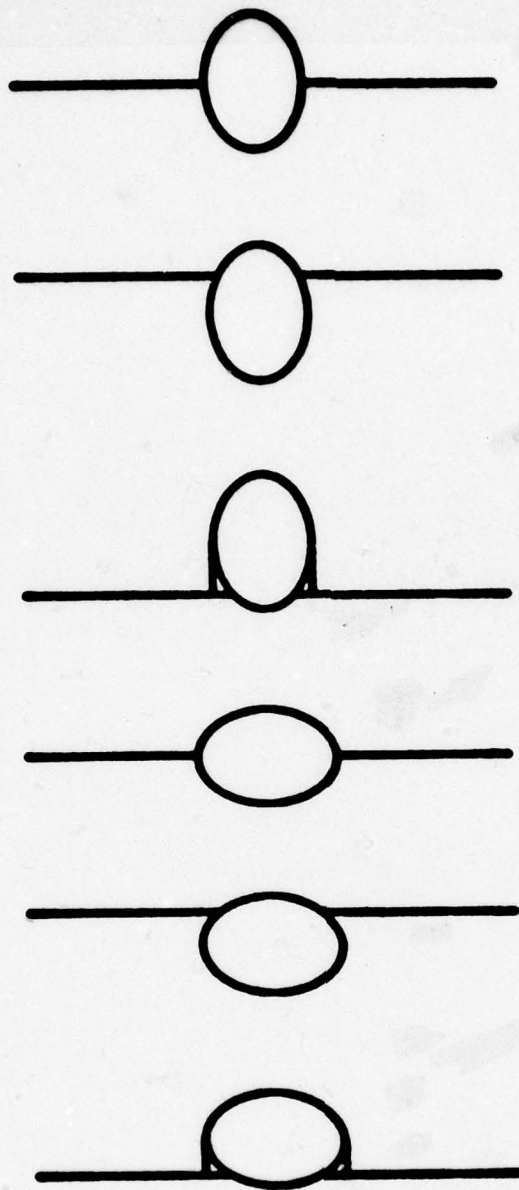
12

Figure 8. Fuselage and wing geometry for theoretical
aircraft model looking from the front. The
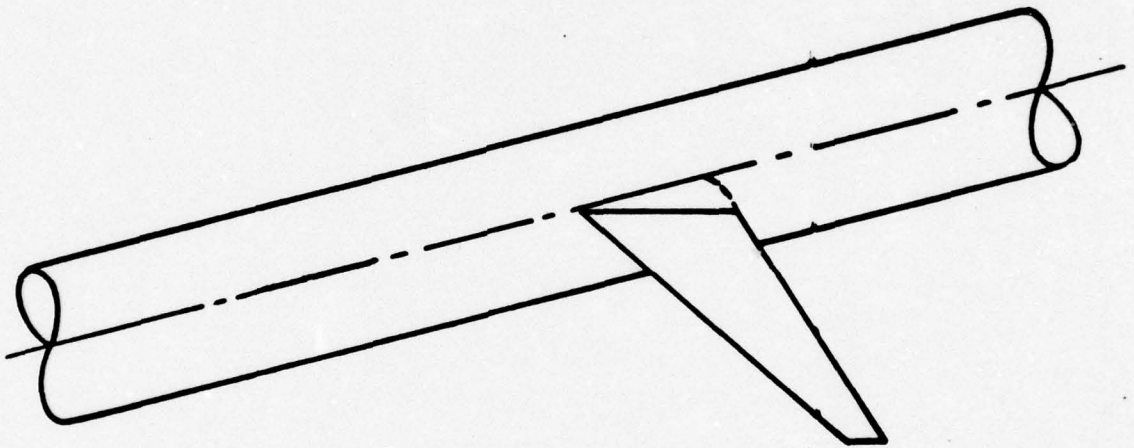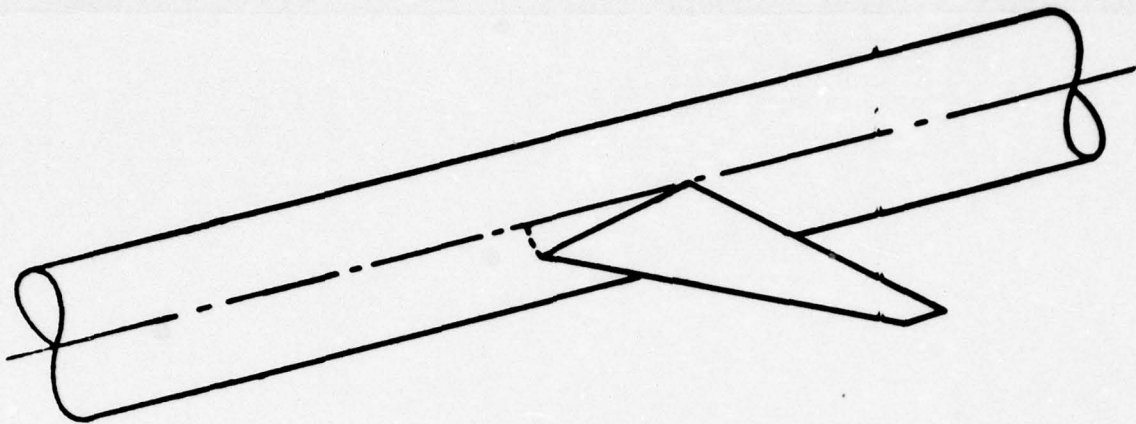antenna is always mounted on top of the
models.

13

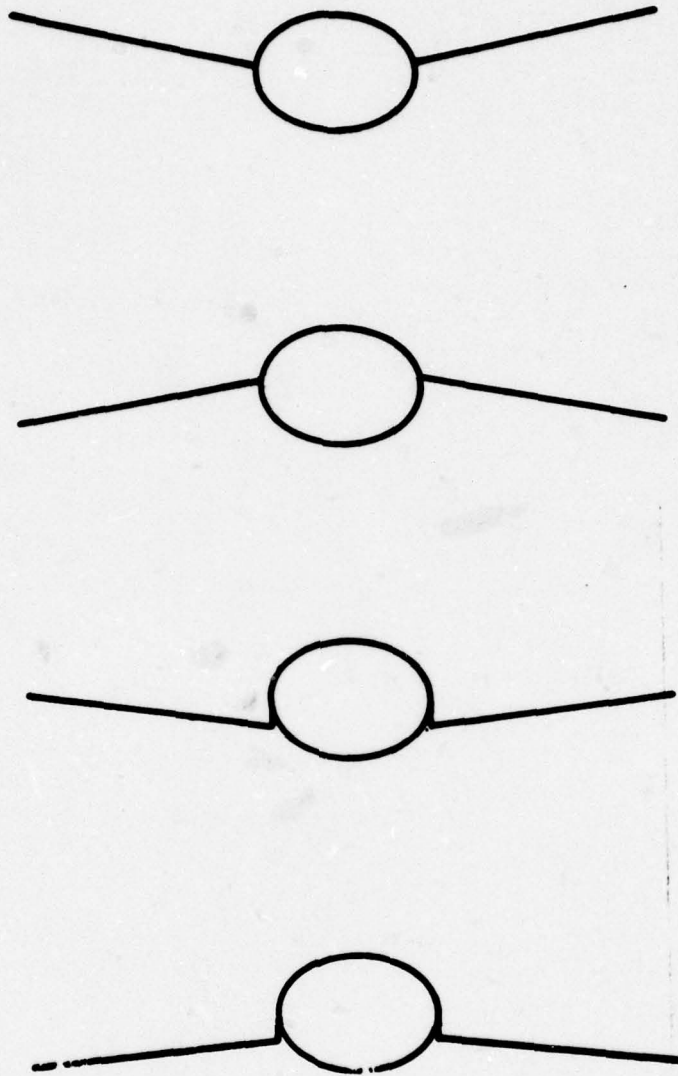Figure 9(a). Illustration of wings tilted forward and backward.

14

Figure 9(b). Illustration of wings tilted sideways.
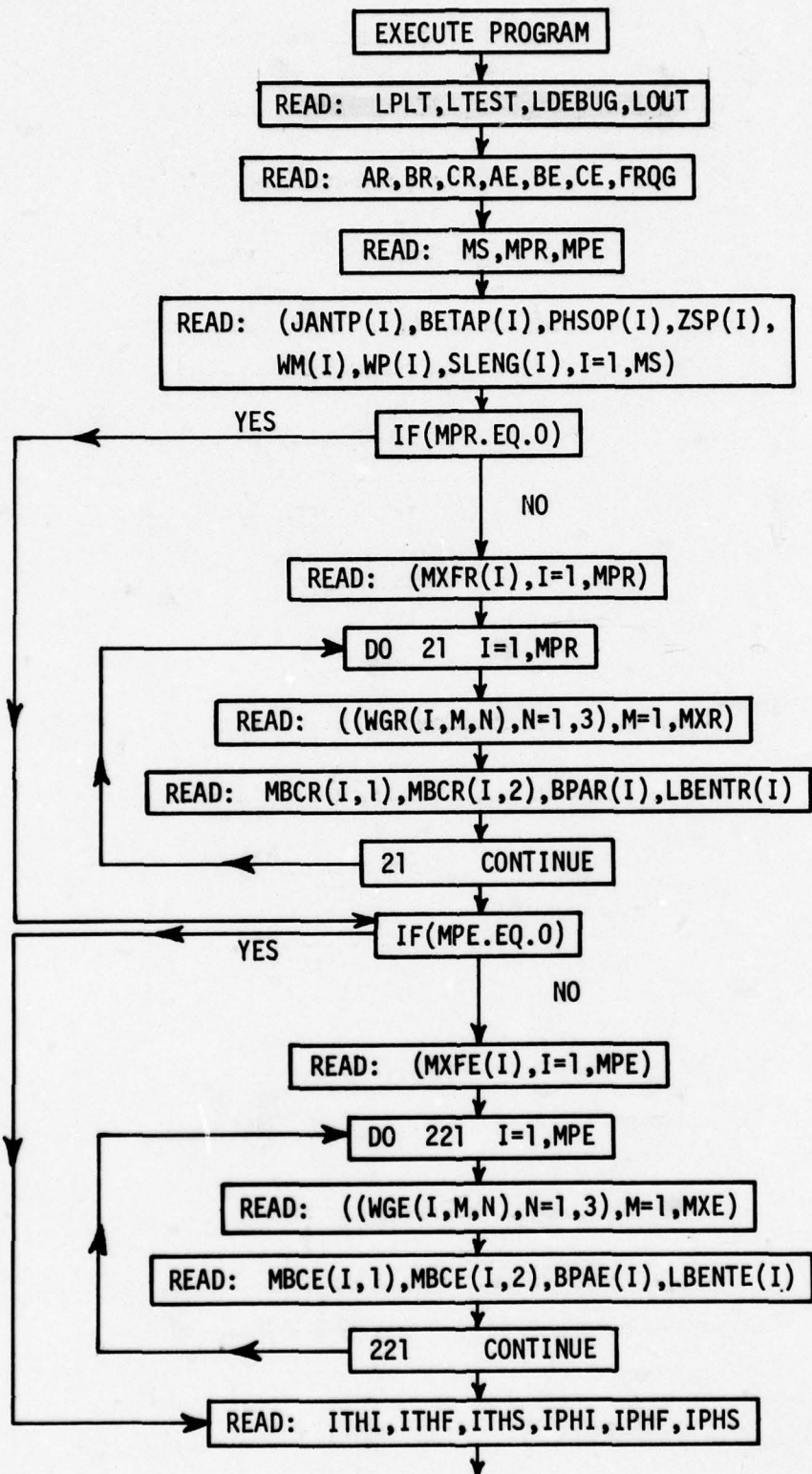
15

III. DEFINITION OF INPUT DATA

As stated earlier, the input data associated with the aircraft geometry is defined by the two composite ellipse models (roll and elevation). Each of these models has its own coordinate system as shown in Figure 6. All linear dimensions are iven in terms of inches and all angular dimensions in degrees. In most cases angular quantities are expressed in terms of theta and phi, the usual spherical coordinates.

It is felt that the maximum usefulness of the computer code can be achieved using it on an interactive computer system. As a consequence, all input data are defined in free format such that the operator need only put commas between the various inputs. This allows one on an interactive terminal to input data without being concerned with the field length associated with a fixed format.

The organization of the input data is illustrated in Table 1. Note that unless indicated otherwise all read statements are made on unit number 5, i.e., READ (5,-), where the "-" symbol refers to free format. In all the following discussions associated with logical variables a "T" will imply true, and an "F" will imply false. The complete words true and false need not be input in that most compilers just consider the first character in determining the state of the logical variable. The following list defines in detail the function associated with each of the input variables.

1.   READ: LPLT, LTEST, LDEBUG, LOUT

   a) LPLT: This is a logical variable defined by T or F. It is used to determine whether a pen plot of results is desired by the operator. If set true, the program plots both the E-theta and E-phi patterns in polar form. In addition if set true, input data must be supplied on unit #8. This data is described later. If set false no data is necessary on unit #8.

   b) LTEST: This is a logical variable defined by T or F. It is used to test the input/output associated with each subroutine. The data, written out on unit #6, are associated with the parameters in the window of the subroutine. They are written out each time the subroutine is called. It is, also, used to insure initial operation of the code. Only one pattern angle is considered and this pattern angle is specified by IPHI (refer to item 11b for its definition).
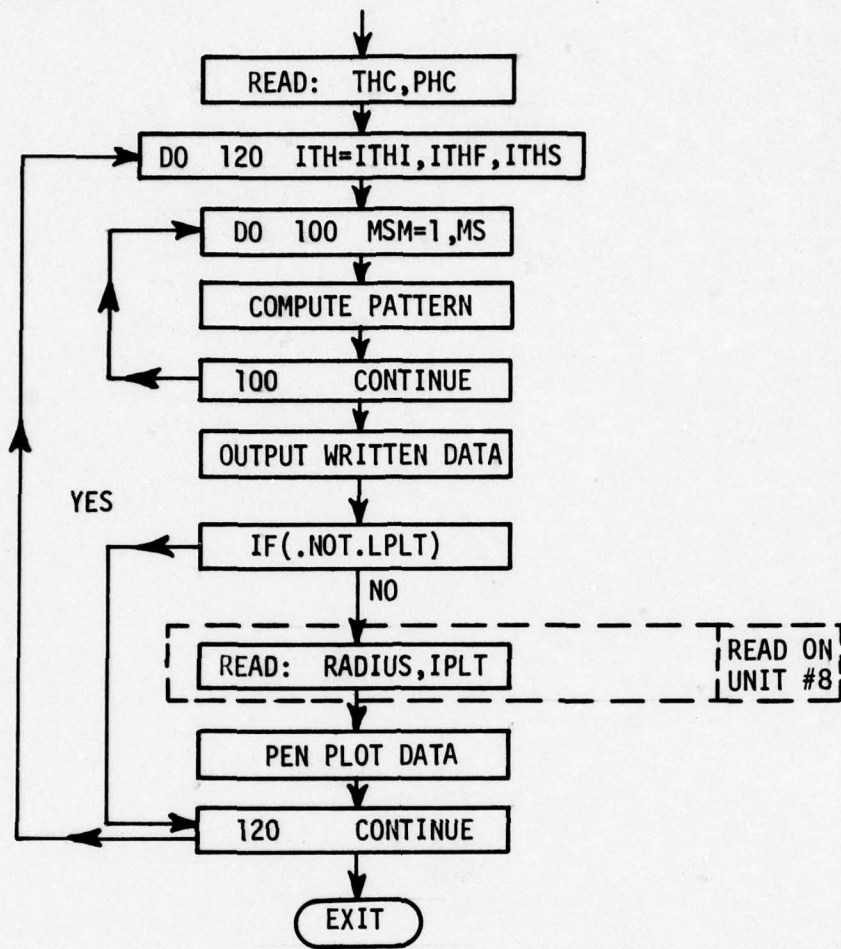   (normally set false)

```
                    ┌─────────────────────┐
                    │  EXECUTE PROGRAM    │
                    └─────────────────────┘
                               │
          ┌────────────────────────────────────────┐
          │ READ:  LPLT,LTEST,LDEBUG,LOUT          │
          └────────────────────────────────────────┘
                               │
          ┌────────────────────────────────────────┐
          │ READ:  AR,BR,CR,AE,BE,CE,FRQG          │
          └────────────────────────────────────────┘
                               │
             ┌──────────────────────────────────┐
             │ READ:  MS,MPR,MPE                 │
             └──────────────────────────────────┘
                               │
       ┌──────────────────────────────────────────────────┐
       │ READ:  (JANTP(I),BETAP(I),PHSOP(I),ZSP(I),       │
       │        WM(I),WP(I),SLENG(I),I=1,MS)              │
       └──────────────────────────────────────────────────┘
                               │
          YES         ┌─────────────────────┐
      ◄───────────────│    IF(MPR.EQ.0)     │
                      └─────────────────────┘
                               │ NO
                  ┌────────────────────────────────┐
                  │ READ:  (MXFR(I),I=1,MPR)       │
                  └────────────────────────────────┘
                               │
                ┌────────────────────────────────┐
                │ DO  21  I=1,MPR               │
                └────────────────────────────────┘
                               │
          ┌──────────────────────────────────────────┐
          │ READ:  ((WGR(I,M,N),N=1,3),M=1,MXR)      │
          └──────────────────────────────────────────┘
                               │
        ┌────────────────────────────────────────────────┐
        │ READ:  MBCR(I,1),MBCR(I,2),BPAR(I),LBENTR(I)   │
        └────────────────────────────────────────────────┘
                               │
                  ┌────────────────────────────────┐
                  │ 21       CONTINUE             │
                  └────────────────────────────────┘
                               │
          YES         ┌─────────────────────┐
      ◄───────────────│    IF(MPE.EQ.0)     │
                      └─────────────────────┘
                               │ NO
                  ┌────────────────────────────────┐
                  │ READ:  (MXFE(I),I=1,MPE)       │
                  └────────────────────────────────┘
                               │
                ┌────────────────────────────────┐
                │ DO  221  I=1,MPE              │
                └────────────────────────────────┘
                               │
          ┌──────────────────────────────────────────┐
          │ READ:  ((WGE(I,M,N),N=1,3),M=1,MXE)      │
          └──────────────────────────────────────────┘
                               │
        ┌────────────────────────────────────────────────┐
        │ READ:  MBCE(I,1),MBCE(I,2),BPAE(I),LBENTE(I)   │
        └────────────────────────────────────────────────┘
                               │
                  ┌────────────────────────────────┐
                  │ 221      CONTINUE             │
                  └────────────────────────────────┘
                               │
        ┌────────────────────────────────────────────────┐
        │ READ: ITHI,ITHF,ITHS,IPHI,IPHF,IPHS           │
        └────────────────────────────────────────────────┘
                               │
                               ▼
```

17

```
        READ:  THC,PHC

DO  120  ITH=ITHI,ITHF,ITHS

    DO  100  MSM=1,MS

    COMPUTE PATTERN

100        CONTINUE

OUTPUT WRITTEN DATA

YES

IF(.NOT.LPLT)

NO

READ:  RADIUS,IPLT          READ ON
                            UNIT #8

PEN PLOT DATA

120        CONTINUE

        EXIT
```

TABLE I

Block Diagram of Input Data and
Main Program Organization

18

c) LDEBUG: This is a logical variable defined by T or F. It is used to output debug data on unit #6. If set true, the program prints out results pertinent to its internal operations. These data can, then, be compared with previous data which are known to be correct. It is, also, used to insure initial operation of the code. Only one pattern angle is considered and this angle is specified by IPHI (refer to item 11b for its definition). (normally set false)

d) LOUT: This is a logical variable defined by T or F. It is used to output data associated with each of the scattering terms. It is used to identify which section of the code is having problems. It is, also, used to insure initial operation of the code. (normally set false)

2. READ: AR,BR,CR,AE,BE,CE,FRQG

a) AR,BR,CR: These are real variables used to define the roll model ellipse in inches. The definition of these variables is shown in Figure 6a.

b) AE,BE,CE: These are real variables used to define the elevation ellipse model in inches. The definition of these variables is shown in Figure 6b.

c) FRQG: This is a real variable used to define the frequency in gigahertz.

3. READ: MS,MPR,MPE

a) MS: This is an integer variable. It is used to specify the number of antenna elements used in the computation. Presently, $1 \le MS \le 9$.

b) MPR: This is an integer variable. It is used to specify the number of plates employed in the simulation of the wings and horizontal stabilizers. This data is used in conjunction with the roll model simulation illustrated in Figure 6a. Presently, $0 \le MPR \le 8$.

c) MPE: This is an integer variable. It is used to specify the number of plates employed in the simulation of the nose section and vertical stabilizer. This data is used in conjunction with the elevation simulation illustrated in Figure 6b. Presently, $0 \le MPE \le 8$.

19

4. READ: (JANTP(I),BETAP(I),PHSOP(I),ZSP(I),WM(I),WP(I),SLENG(I),I=1,MS)

a) JANTP(I): This is a dimensioned integer variable. It is used
    to define the Ith antenna type as follows:

    1 = infinitesimal slot
    2 = arbitrary length slot with cosine distribution
    3 = infinitesimal monopole
    4 = arbitrary length monopole with cosine distribution
    Presently, $1 \leq I \leq 9$.

b) BETAP(I): This is a dimensioned real variable. It is used to
    define the slot angle on the Ith antenna in degrees
    relative to the aircraft axis. For example, an axial
    slot is defined with BETAP=0. and a circumferential slot
    with BETAP=90.. It is always input but only used if
    JANTP = 1 or 2. Presently, $1 \leq I \leq 9$.

c) PHSOP(I): This is a dimensioned real variable. It is used to specify
    the Ith antenna location in the cross-sectional view of the
    aircraft as shown in Figure 10. It is an angular quantity
    given in degrees. Presently, $1 \leq I \leq 9$ and $-90. \leq PHSOP \leq 90$.

d) ZSP(I): This is a dimensioned real variable. It is used to
    specify the Ith antenna location in the profile view
    relative to the reference coordinates as shown
    in Figure 10. It is a linear dimension given in
    inches. Presently, $1 \leq I \leq 9$.

e) WM(I),WP(I): These are dimensioned real variables. They are
    used to specify the magnitude and phase, respectively,
    of the excitation on the Ith antenna element. Note
    that WP is the phase in degrees. Presently, $1 \leq I \leq 9$.

f) SLENG(I): This is a dimensioned real variable. It is used to
    specify the length of the antenna element. Note it
    is input in wavelengths. The length is always input,
    but it is only used if JANTP(I)=2 or 4. Presently,
    $1 \leq I \leq 9$.

5. READ; (MXFR(I),I=1,MPR)

a) MXFR(I): This is a dimensioned integer variable. The mag-
    nitude of MXFR(I) defines the number of corners
    associated with the Ith plate. If MXFR(I) is
    positive, then the first and last corner attach to the
    fuselage. If MXFR(I) is negative, then only the first
    corner attaches to the fuselage. Normally MXFR is
    positive. Note MXFR(I) just refers to the roll model
    plates. Presently, $1 \leq I \leq 8$.

20
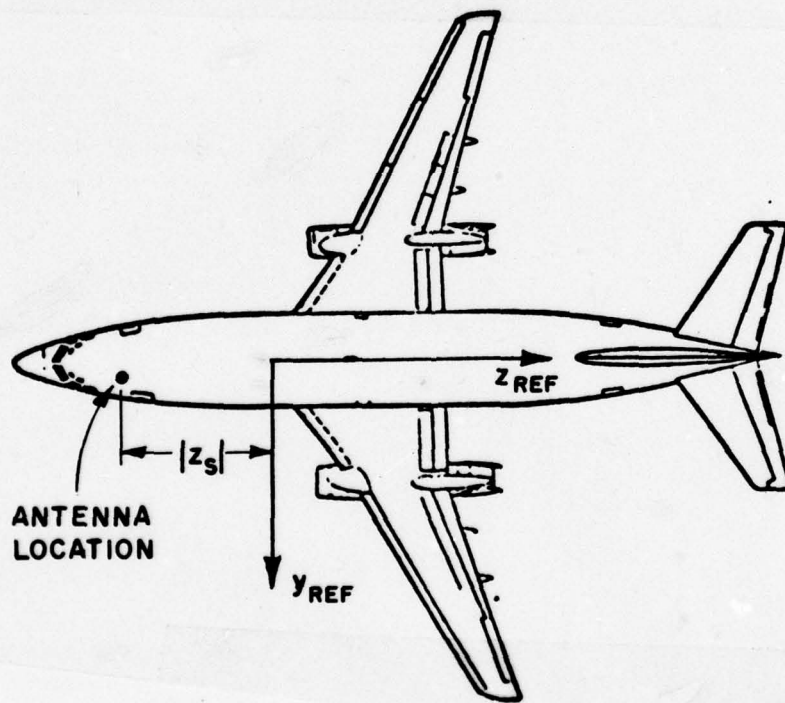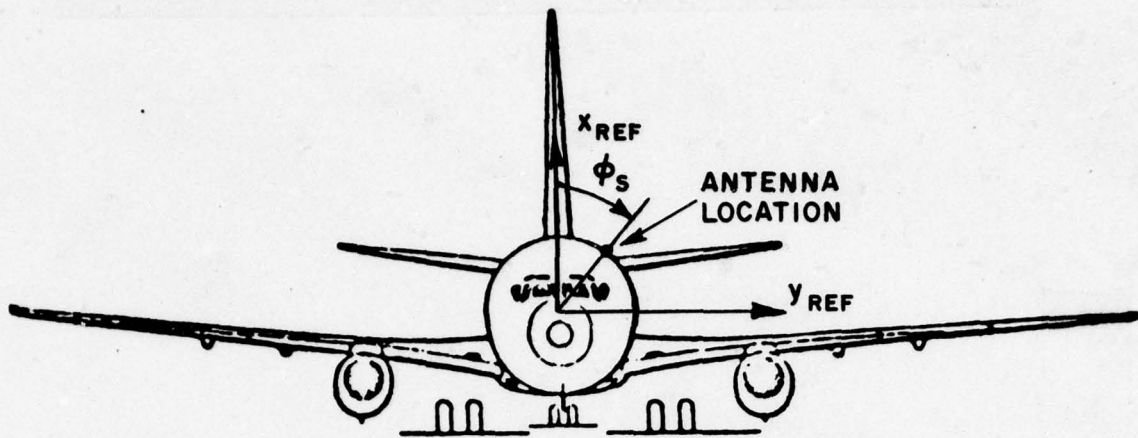
Figure 10. Definition of the source location for computer code. Note that PHSOP = ϕ_S and ZSP = $- |Z_S|$ in the above drawings.

21

6.   READ: ((WGR(I,M,N),N=1,3),M=1,|MXFR(I)|)

   a) WGR(I,M,N):   This is a triply dimensioned real variable. It is
                     used to define the corner locations (in inches) of
                     the Ith plate in the roll model coordinates as
                     shown in Figure 6a. Note that N=1,2,3 specifies
                     the x,y,z coordinates respectively of the Mth
                     corner. Presently, $1 \leq I \leq 8$, $1 \leq M \leq 10$ and
                     $1 \leq N \leq 3$.

**Note that more information about the corner location definition is given
in the next section.**

   To input the bent plate geometry into the computer program, two options
are provided. One is to input the I-th flat plate geometry with LBENTR(I) =
F and specify a desired bend angle by BPAR(I). The corners [MBCR(1,1) and
MBCR(1,2)] about which the plate is to be bent by the computer code should
also be specified and are illustrated in Figure 11(a). The computer program
will then bend the plate to give the desired geometry as seen in Figure 11b.
The second way is to input directly the desired bent plate geometry into the
computer program with LBENTRI(I) = T and the wing is input as a bent plate.
In this case, the computer program will bypass the wing bending section since
the plate is already bent and proceed as usual. The quantities LBENTR, BPAR,
MBCR, ... etc are input parameters in the computer program as described below.

7.   READ: MBCR(I,1),MBCR(I,2),BPAR(I),LBENTR(I)

   a) MBCR(I,1),MBCR(I,2): These are dimensional integer variables.
       They are used to define the first and last corners, respectively,
       about which the Ith plate is to be bent. Thus, if a plate is to
       have a bend, then it should be defined such that two corners
       correspond to the bend line. Note that if the plate is flat
       (no bend), MBCR(I,1) = MBCR(I,2) =|MXFR(I)|. This input is for
       roll model plates only. Presently, $1 \leq I \leq 8$.

   b) BPAR(I): This is a dimensioned real variable. It is used to
       specify the bend angles in degrees of the Ith plate. Note that
       if the plate is flat, BPAR(I) = 180.. Presently, $1 \leq I \leq 8$.

   c) LBENTR(I): This is a dimensioned logical variable defined by
       T or F. It is used to specify to the code whether the Ith plate
       is already bent (T) or not (F). If LBENTR(I) = F, then the Ith
       plate is bent by the computer code about the corners MBCR(I,1)
       and MBCR(I,2) to the angle BPAR(I). If the Ith plate is flat,
       then LBENTR(I) = T. Presently, $1 \leq I \leq 8$.

Note that the bent plate may be used in the roll model to simulate the bent
up wing on the F-4 or flaps.

22
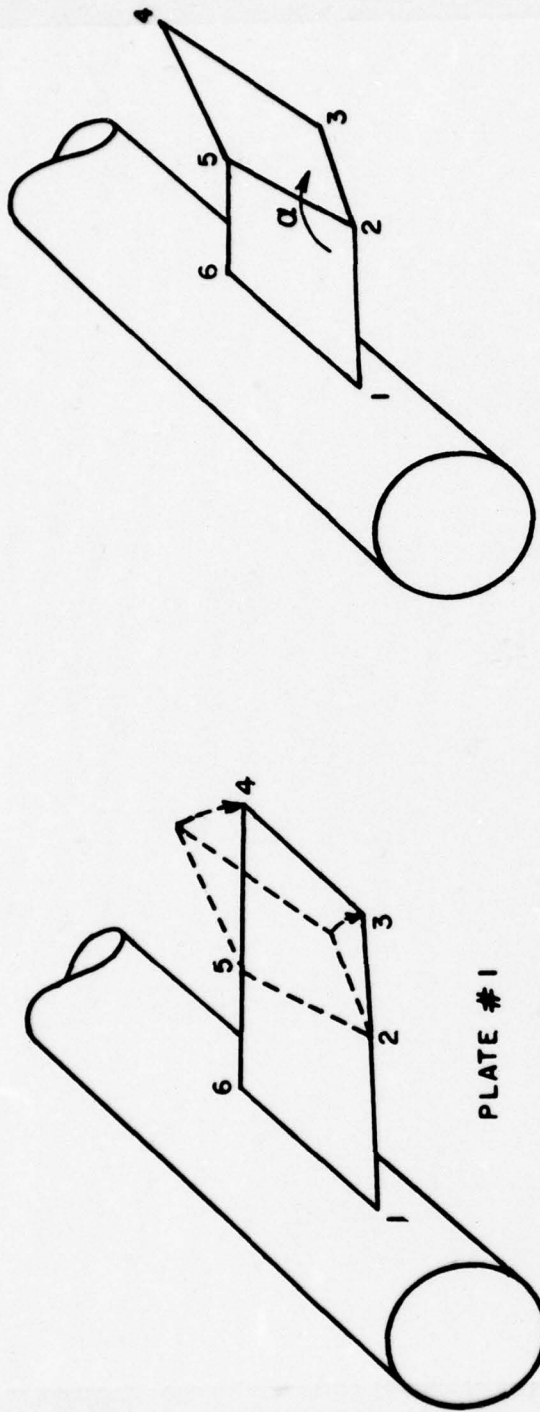
PLATE #1

(a)

(b)

Figure 11. Illustration of different means of inputting bent plate data with MBCR(1,1) = 2, MBCR(1,2) = 5, and BPAR(1) = $\alpha°$.

a) Illustration of geometry with LBENTR(1) = F. The data for the wing is input as though the wing were pressed flat without a bend. The program then bends the plate about corners 2 and 5 and produces the geometry shown in (b).

b) Illustration of geometry with LBENTR(1) = T. The data for the wing is input as though the wing were already bent. The program, then, bypasses the bend section of the code.

23

8. READ: (MXFE(I), I=1, MPE)

a) MXFE(I): This is a dimensioned integer variable. The magnitude of MXFE(I) defines the number of corners associated with the Ith plate. If MXFE(I) is positive, then both the first and last corner of the Ith plate attach to the fuselage. IF MXFE(I) is negative, then only the first corner attaches to the fuselage. Note that MXFE(I) just refers to the elevation model plates. It is normally used as a negative quantity to simulate the vertical stabilizer as shown in Figure 6b. Presently, $1 \le I \le 8$.

9. READ: ((WGE(I,M,N), N=1,3), M=1,|MXFE(I)|)

a) WGE(I,M,N): This is a triply dimensioned real variable. It is used to define the corner locations (in inches) of the Ith plate in the elevation model coordinates as shown in Figure 6b. Note that N=1,2,3 specifies the x,y,z coordinates, respectively, of the Mth corner. Presently, $1 \le I \le 8$, $1 \le M \le 10$, and $1 \le N \le 3$.

Note that more information about the corner location definition is given in the next section.

10. READ: MBCE(I,1), MBCE(I,2), BPAE(I), LBENTE(I)

a) MBCE(I,1), MBCE(I,2): These are dimensioned integer variables. They are used to define the first and last corner, respectively, about which the Ith plate is to be bent. Thus, if a plate is to have a bend, then it should be defined such that these two corners correspond to the bend line. Note that if the plate is flat (no bend), MBCE(I,1)=MBCE(I,2)=|MXFE(I)|. This input is for the elevation model plates only. Presently, $1 \le I \le 8$.

b) BPAE(I): This is a dimensioned real variable. It is used to specify the bend angle in degrees of the Ith plate in the elevation model. Note that if the plate is flat, BPAR(I)=180. Presently, $1 \le I \le 8$.

c) LBENTE(I): This is a dimensioned logical variable defined by T or F. It is used to specify to the code whether the Ith plate is already bent (T) or not (F). If LBENTE(I)=F, then the Ith plate is bent by the computer code about the corners MBCE(I,1) and MBCE(I,2) to the angle BPAE(I). If the Ith plate is flat, then LBENTE(I)=T. Presently, $1 \le I \le 8$.

The next two read statements are associated with the conical pattern desired during execution of the program. The pattern axis is defined by the spherical angles (THC,PHC) as illustrated in Figure 12. These angles define a radial vector direction which points in the direction of the pattern axis of rotation. These angles actually set-up a new coordinate system in relation to the fixed reference coordinates. The new cartesian
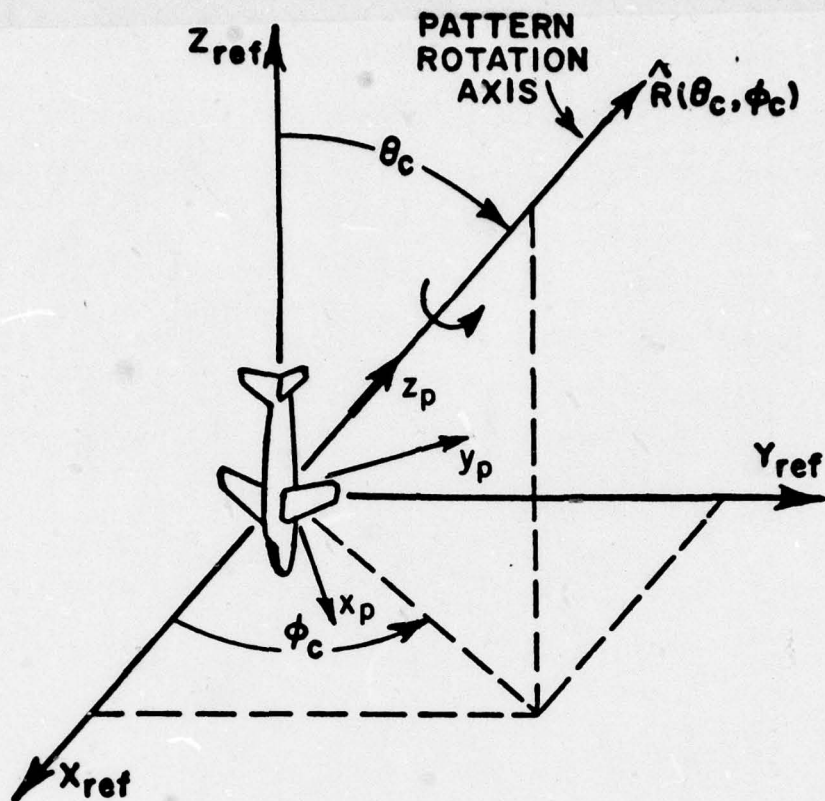
Figure 12.   Illustration of the rotation angle (θ_c, ϕ_c)
in spherical coordinate system.

coordinates defined by the subscript "p" are found by first rotating
about the z-axis the angle PHC and, then, about the y-axis the angle
THC. The pattern is taken in the "p" coordinate system in terms of the
spherical angles. The theta angle of the pattern taken about the
z_p-axis is defined by THP, which is input to the code in terms of ITHI,
ITHF, ITHS. The phi angle is defined in the "p" coordinate system in
terms of IPHI, IPHF, IPHS. These angles are input in terms of integer
variables so that the data can be stored in associated arrays. In the
present form the program will, then, compute any conical pattern or a
series of conical patterns about an operator defined pattern axis.

11. READ: ITHI, ITHF, ITHS, IPHI, IPHF, IPHS

   a) ITHI, ITHF, ITHS: These are integer variables used to define
       angles in degrees. They are, respectively, the initial, final,
       and incremental values of the theta pattern angle. Note that
       for each theta angle a complete pattern is taken in terms of
       the phi pattern angles.

25

b) IPHI, IPHF, IPHS: These are integer variables used to define angles in degrees. They are, respectively, the initial, final and incremental values of the phi pattern angle. Note that for each theta a complete phi pattern is taken.

12. READ: THC, PHC

a) THC,PHC: These are real variables. They are input in degrees and define the axis of rotation about which various conical patterns will be computed.

This completes the input data necessary to compute the desired patterns. If the operator wishes to generate a set of pen plots (LPLT=T), then the following data must input on unit #8.

1. READ: RADIUS, IPLT

a) RADIUS: This is a real variable. It is used to specify the radius of the outer circle of the polar plot in inches.

b) IPLT: This is an integer variable. It is used to specify the type of plot desired:

$$1 = \text{field plot}$$
$$2 = \text{power plot}$$
$$3 = \text{dB plot.}$$

Note that all plotted patterns are normalized such that the maximum value corresponds to the outer circle. The dB plot is drawn with each circle corresponding to 10 dB.

Note that both the E-theta and E-phi patterns will be plotted if LPLT=T.

26

IV. SIMULATION OF BOEING 737 AIRCRAFT

To begin any simulation of an aircraft, one needs to start with a set of scale model drawings. For our purposes, Jane's book [8] "All the World's Aircraft" is most appropriate in that it provides a line drawing for each aircraft. The line drawings for the 737 aircraft are shown in Figure 13 along with our simulation models.

To begin the simulation procedure, one finds the elliptic parameters for both the roll and elevation models. The elliptic curves should simulate the fuselage surface as accurately as possible near the antenna location. Using the best-fit ellipse routine given in Appendix A, and the scale model drawings shown in Figure 13, the following values of a 1/20 scale model of the 737 aircraft were obtained:

$$a_r = 65.86" \qquad a_e = 58.72"$$
$$b_r = 43.3" \qquad b_e = 308.56"$$
$$c_r = 43.3" \qquad c_e = 1307.04" \; .$$

The above values were scaled and used to plot the simulation models shown in Figure 13. Note that the roll model ellipse appears to be incorrect based on Figure 13b. However, one must recall that the cross-section at the antenna position is being simulated and not the cross-section in the middle of the aircraft.

Once the ellipse dimensions are specified the plates are added to the model. Let us first consider the roll model in which case one wishes to simulate the wings and horizontal stabilizers. From the front view of the aircraft in Figure 13b, one can determine the x_r values of the plates. Note that only the wings are considered in this case. The horizontal stabilizers are so far away from the antenna that they can be neglected. For the wings, $x_r=0$ in this case. From the top view of the aircraft, the y_r and z_r dimensions of the wings are obtained as shown in Figure 13c. Using this information the following input data is obtained:

Corner #	wing #1	wing #2
1	$x_r=0"$, $y_r= 43.3"$, $z_r = 56.54"$	$x_r=0"$, $y_r=-43.3"$, $z_r=233.54"$
2	$x_r=0"$, $y_r=536.93"$, $z_r=316.14"$	$x_r=0"$, $y_r=-536.93"$, $z_r=379.86"$
3	$x_r=0"$, $y_r=536.93"$, $z_r=379.86"$	$x_r=0"$, $y_r=-536.93"$, $z_r=316.14"$
4	$x_r=0"$, $y_r=43.3"$, $z_r=233.54"$	$x_r=0"$, $y_r=-43.3"$, $z_r=56.54"$

Note that the data is input counter clockwise looking at the top view of the aircraft as presented in Figure 13c. The data is for a 1/20 scale model of the 737 aircraft so that the data for the wings as taken from Figure 13

is multiplied by the appropriate scale factor. Finally, one should realize
that the program attaches the wings (or plates) to the cylinder so the user
need not worry about attaching perfectly to the cylinders.

Next, let us consider the data used to simulate the nose section and
vertical stabilizer. Before defining the nose section plate, one must
identify the location of the radome. The radome is constructed of low
dielectric constant material such that it can be considered to be free
space in the calculation. Note that the radome line is easily identi-
fiable in Figure 13a and c. The x_e and z_e dimensions of the nose plate
is obtained from the side view as shown in Figure 13a. The top view is
used to determine the z_e dimensions of the nose section plate. In our
simulation, the plate geometry corresponds to the maximum dimensions of
the nose section as shown in Figure 13c. The data generated for the nose
section plate is as follows:

Corner	nose section plate
1	$x_e=0"$, $y_e=308.56"$, $z_e=-31.585"$
2	$x_e=-5.6"$ $y_e=321.6"$, $z_e=-27.07"$
3	$x_e=-5.6"$, $y_e=321.6"$, $z_e=27.07"$
4	$x_e=0"$, $y_e=308.56"$, $z_e=31.585"$

Again recall that the above data is for a 1/20 scale model of the 737
aircraft.   This scale model is used so that the data can be compared
with scale model measurements as shown later.

Since the antenna is assumed to be on or near the center line of the
aircraft, one must take into account the finite width of the vertical
stabilizer. As can be seen in Figure 13c, the vertical stabilizer has
some width which will cause shadowing in the aft portion of the pattern.
In order to simulate this width in our model of the aircraft, a bent plate
approximation is employed as shown in Figure 6b. The dominant features
of the vertical stabilizer which must be preserved are the width and leading
edge geometry. The width of the vertical stabilizer is given in the top
view of the aircraft as shown in Figure 13c. The x_e and y_e dimensions of
the vertical stabilizer are obtained from the side view as shown in Figure
13a; whereas, the z_e components are taken from Figure 13c. Using this
criterion, the following data is obtained:

28
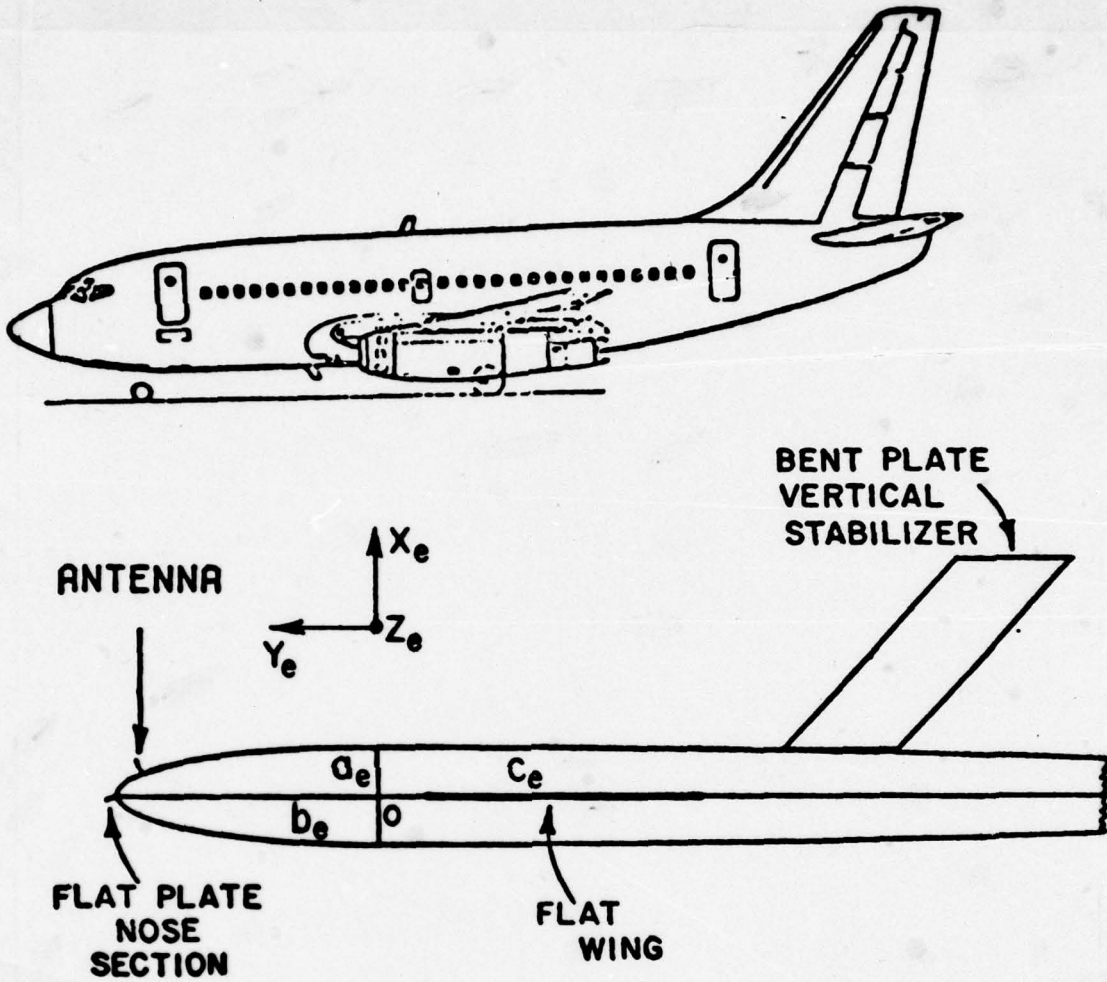
Figure 13(a). Computer simulated model for the fuselage profile of a Boeing 737 aircraft (side view). The antenna is located at station 220 on top of the fuselage.

29
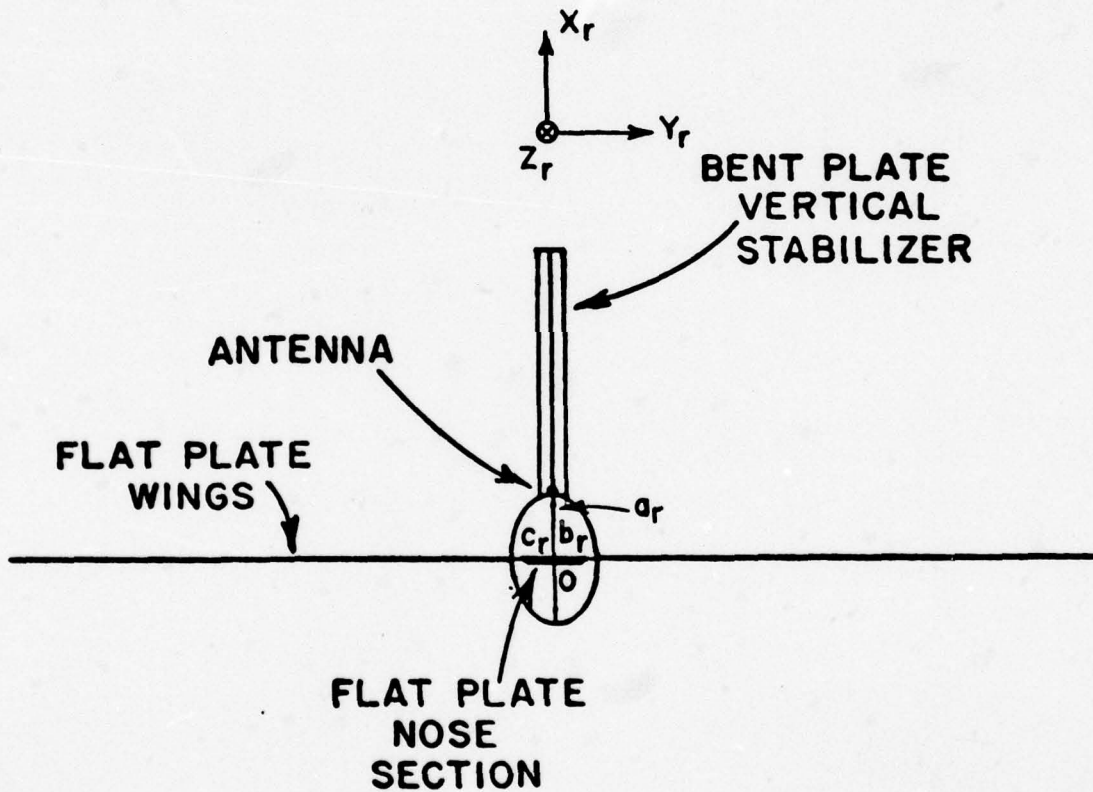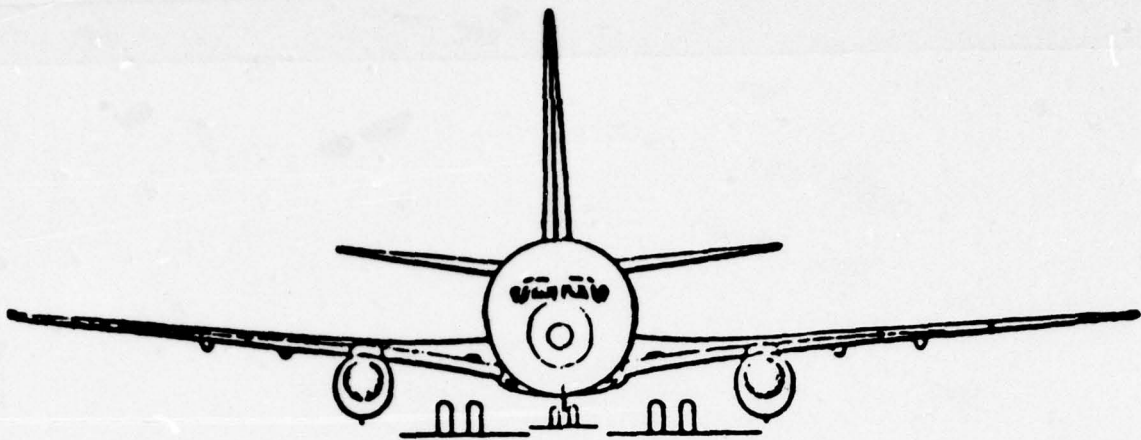
Figure 13(b). Computer simulated model for the cross-section (at antenna location) of a Boeing 737 aircraft (front view). The antenna is located at station 220 on top of the fuselage.

30
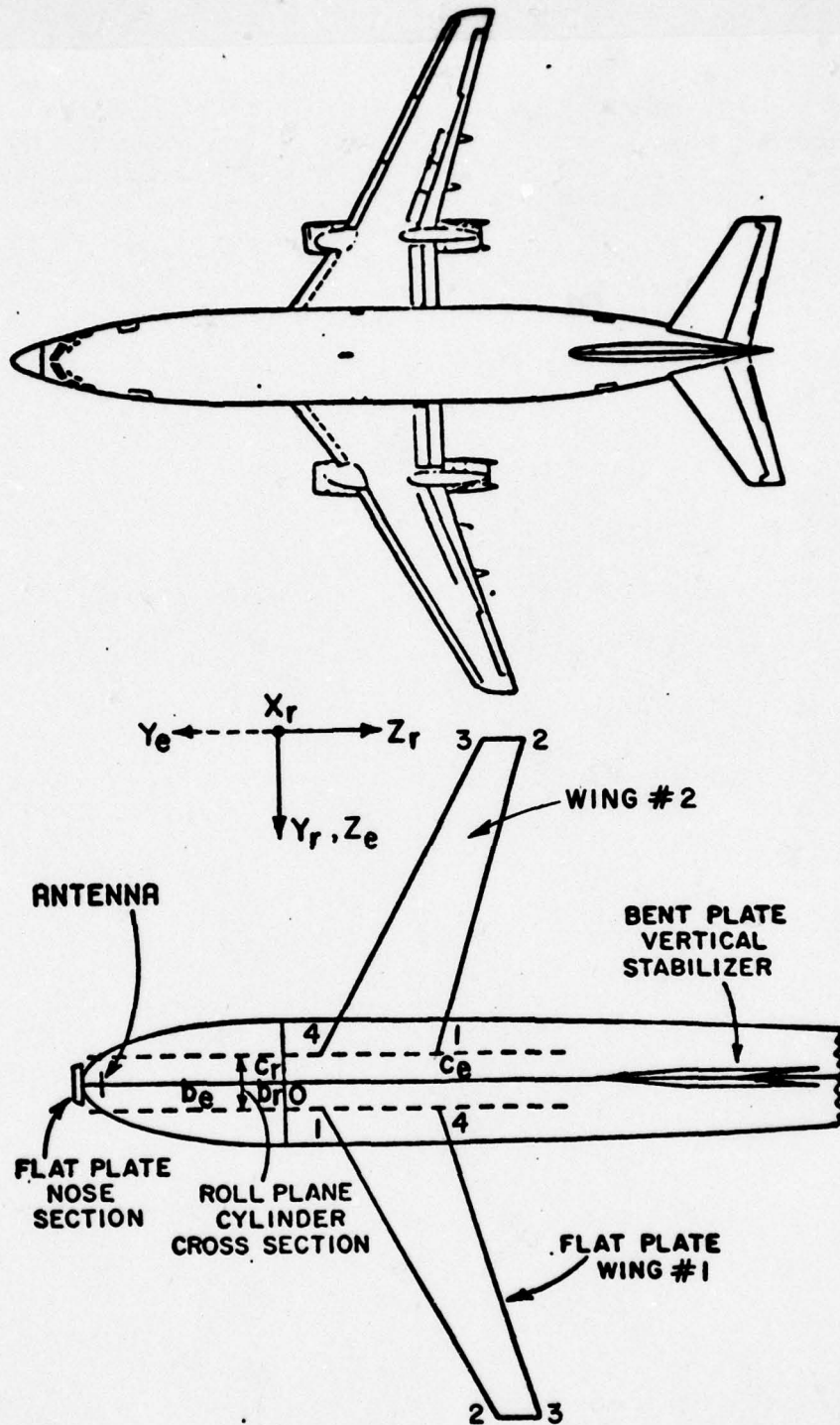
Figure 13(c). Computer simulated model for a Boeing 737 aircraft (top view). The antenna is located at station 220 on top of the fuselage.

31

Corner #	vertical stabilizer plate
1	$x_e = 56.645"$, $y_e = -478.4"$, $z_e = 0"$
2	$x_e = 56.645"$, $y_e = -613.76"$, $z_e = 8.25"$
3	$x_e = 284.147"$, $y_e = -819.056"$, $z_e 8.25"$
4	$x_e = 284.147"$, $y_e = -683.696"$, $z_e = 0"$
5	$x_e = 284.147"$, $y_e = -819.056"$, $z_e = -8.25"$
6	$x_e = 56.645"$, $y_e = -613.76"$, $z_e = -8.25"$

Note that a bent plate is used in this case with the bend already defined such that LBENTE(2)=T. Further, the bend is between corners #1 and #4 and at an angle of 348.58°. As can be seen in Figure 13, this simulation provides a good representation of the leading edge of vertical stabilizer as well as its width.

The only remaining aspect is the location of the antenna on the aircraft simulation model. Again using the scale model drawing of Figure 13, one can determine the actual location of the antenna on the scale model drawings. This data can, then, be transposed to the simulation drawings. Once on the simulation drawings, the antenna location is defined by PHSOP = $\tan^{-1}(y_r/x_r)$, where x_r, y_r defines the antenna location in the roll coordinates as shown in Figure 13b. The ZSOP dimension is obtained from the side view as shown in Figure 13a and is equal to the z_e dimension associated with the antenna location.

Using the above procedure a series of examples were studied to illustrate the various aspects of the computer code. These examples are presented in the next section.

V. APPLICATION OF CODE TO SEVERAL EXAMPLES

1. Elevation plane pattern of an axial waveguide mounted on a prolate spheroid is computed. The geometry is illustrated in Figure 14 and the input data is given by

```
T,F,F,F
6.,6.,6.,12.,12.,12.,4.
2,0,0
2,0.,1.05,0.,1.,0.,0.634
2,0.,-1.05,0.,1.,0.,0.634
90,91,2.0,360,2
90.,90.
```

The axial waveguide is simulated by two infinitesimally wide slots which are 0.634λ long. The elevation pattern is shown in Figure 5.
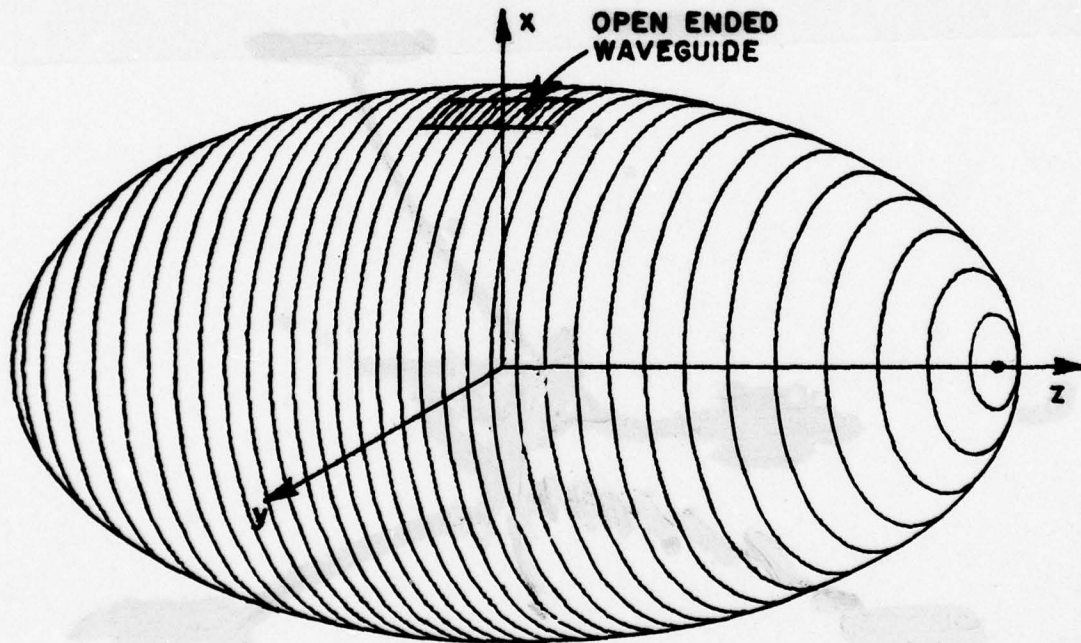
Figure 14. Waveguide antenna mounted on a prolate spheroid.

33

2. Roll and elevation patterns are computed for an axial waveguide, circumferential waveguide, and $\lambda/4$ monopole mounted at two locations on a KC-135 as shown in Figure 15. The input data is as follows:

```
T,F,F,F
3.,3.,3.,3.75,8.,80.,34.92 -  -  -  -  -  -  - ⎫
1,2,2                                           ⎬  INSERT #1
4,0.,0.,8.34,1.,0.,0.25   -  -  -  -  -  -  -  - ⎭
4,4
-1.,3.,12.31
-1.,28.5,36.41
-1.,28.5,40.41
-1.,3.,24.61
4,4,180.,T
-1.,-3.,24.61
-1.,-28.5,40.41
-1.,-28.5,36.41
-1.,-3.,12.31
4,4,180.,T
4,-6
1.5,7.35,-1.36039
.775,9.,-1.36039
.775,9.,1.36039
1.5,7.35,1.39039
4,4,180.,T
2.946,-49.492,0.
2.946,-55.672,0.5
14.076,-64.205,0.5
14.076,-58.025,0.
14.076,-64.205,-0.5
2.946,-55.672,-0.5
1,4,351.,T
90.91,5.0,360,2 -  -  -  -  -  -  -  -  -  -  - ⎫
0.,0.                                           ⎬  INSERT #2
       -  -  -  -  -  -  -  -  -  -  -  -  -  -  ⎭
```

where the data for the defined inserts is given with each of the patterns. The roll and elevation patterns are shown in Figures 16-17. In each case the calculated patterns are compared against measured results. The agreement illustrated by these patterns are typical of the accuracy of the solution. Note that the program outputs both an E-theta and E-phi pattern; whereas, only the dominant polarization is plotted in the previous figures. The definition of these terms is given in the next section. In addition, the waveguide in this case is approximated by a set of three infinitesimally wide slots each with a length of .828λ. This must be done to simulate the distribution across the narrow wall of the waveguide. The cosine distribution across the broad wall of the waveguide is simulated by the extended slot (JANTP=2).

34
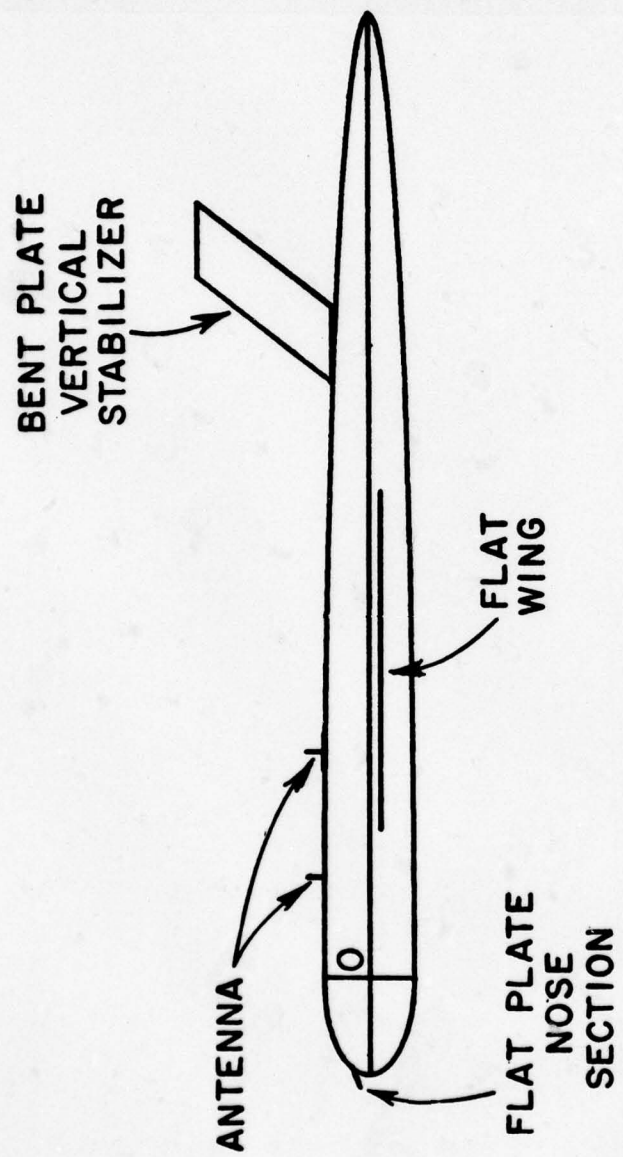
Figure 15a. Computer simulated model for the fuselage profile of a KC-135 aircraft (side view).
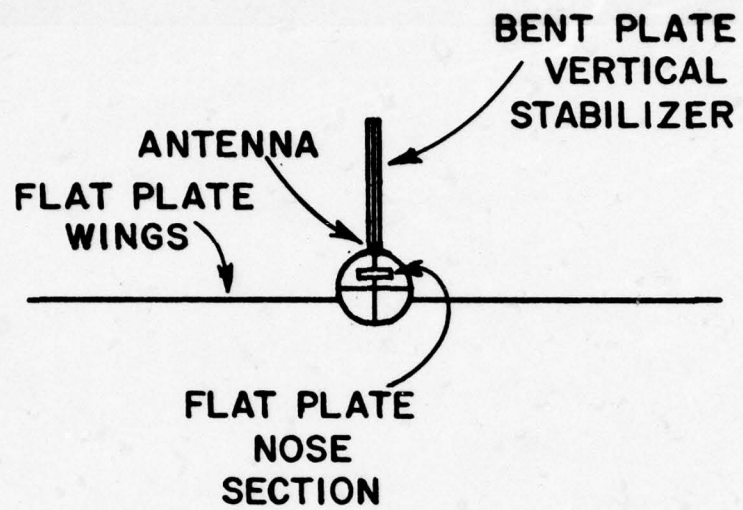
Figure 15b. Computer simulated model for the cross-section
(at antenna location) of a KC-135 aircraft
(front view).
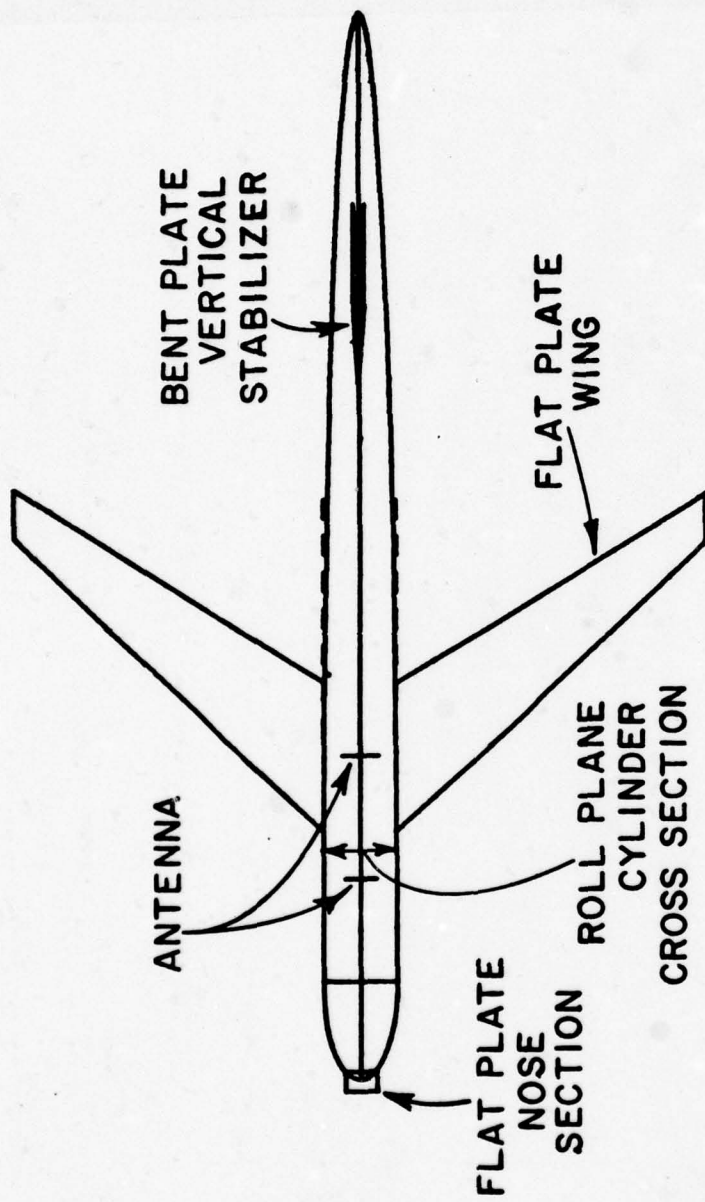
Figure 15c.   Computer simulated model for a KC-135 aircraft (top view).
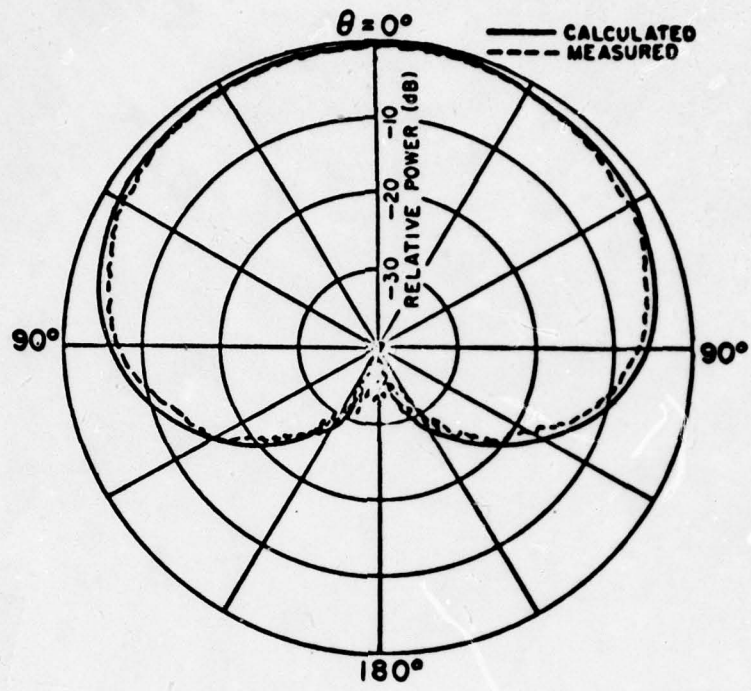
Figure 16a. Roll plane pattern (E_ϕ) for a KA-band axial waveguide forward of the wings.

INSERT #1

3,2,2
2,0.,0.,8.34,1.,0.,,828
2,0.,0.892,8.34,1.,0.,,828
2,0.,-0.892,8.34,1.,0.,,828

INSERT #2

0.,0.
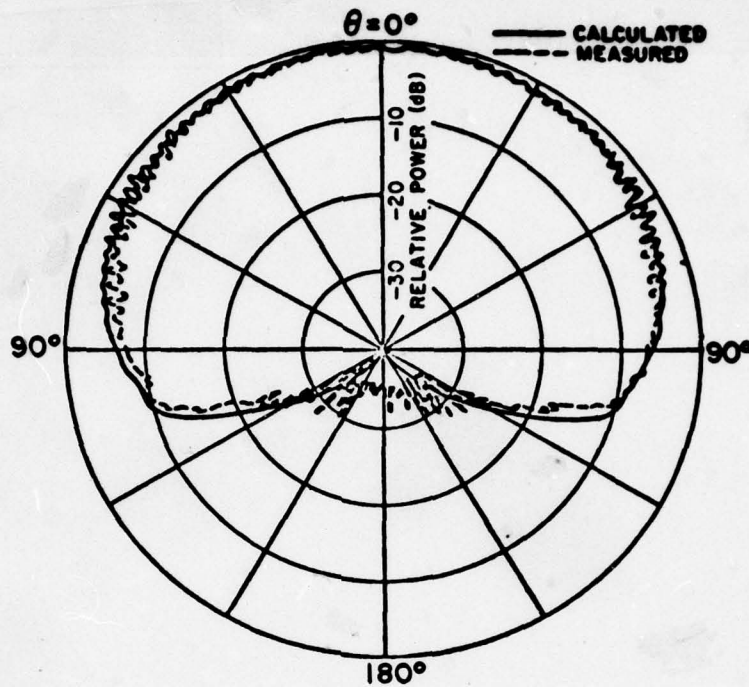
Figure 16b. Roll plane pattern (E_ϕ) for a KA-band axial waveguide above the wings.

INSERT #1

3,2,2
2,0.,0.,18.81,1.,0.,.828
2,0.,.892,18.81,1.,0.,.828
2,0.,-.892,18.81,1.,0.,.828

INSERT #2

0.,0.

39
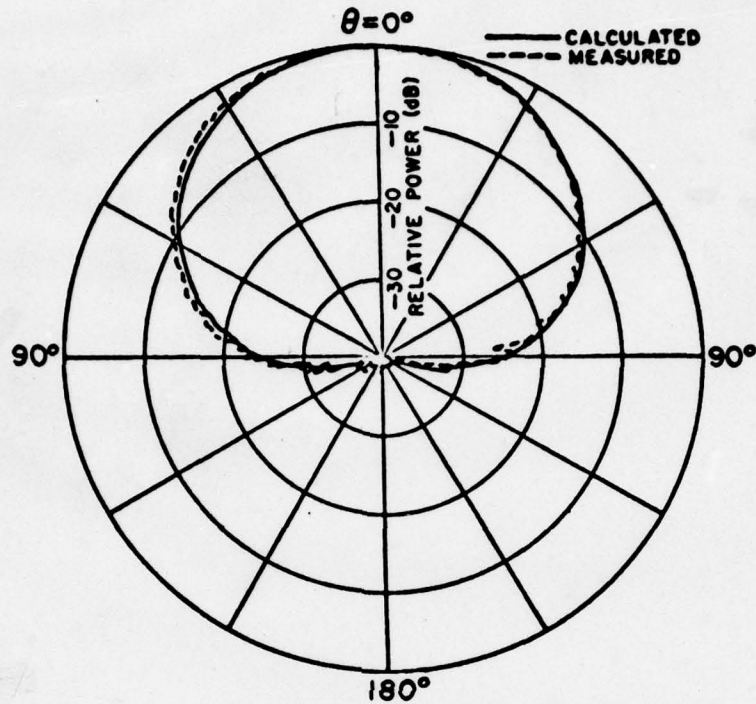
Figure 16c. Roll plane pattern (E_θ) for a KA-band circum-
ferential waveguide forward of the wings.

INSERT #1   INSERT #2

3,2,2   0.,0.
2,90.,0.,8.2933,1.,0.,.828
2,90.,0.,8.34,1.,0.,.828
2,90.,0.,8.3867,1.,0.,.828

40

Figure 16d. Roll plane pattern (E_θ) for a KA-band circum-
ferential waveguide above the wings.

INSERT #1

3,2,2
2,90.,0.,18.7633,1.,0.,.828
2,90.,0.,18.81,1.,0.,.828
2,90.,0.,18.8567,1.,0.,.828

INSERT #2

0.,0.
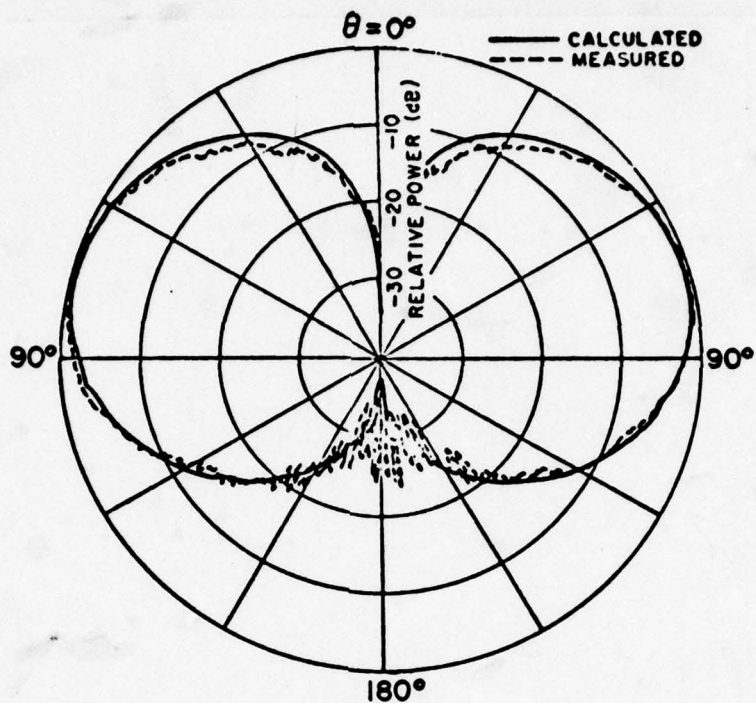
Figure 16e. Roll plane pattern (E_ϕ) for a $\lambda/4$ monopole forward of the wings.

INSERT #1

1,2,2
4,0.,0.,8.34,1.,0.,0.25

INSERT #2

0.,0.
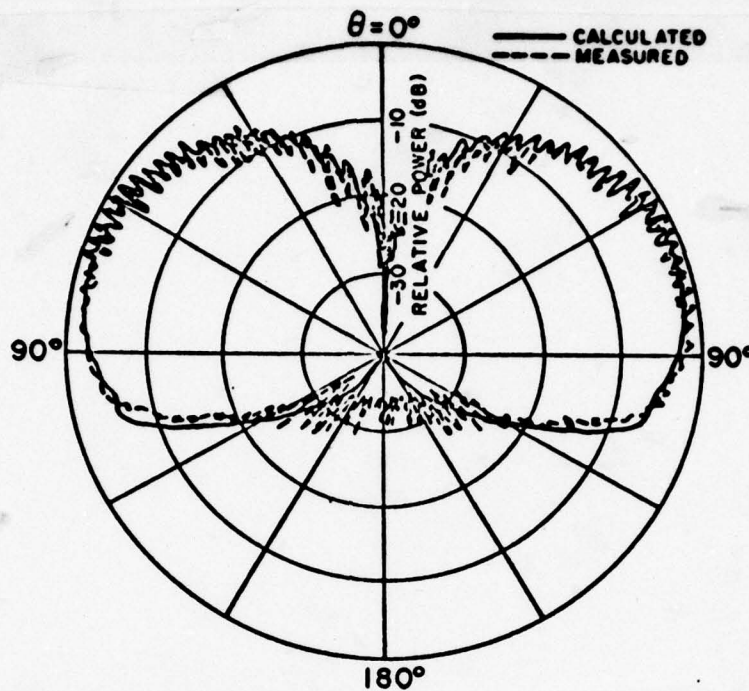
Figure 16f. Roll plane pattern (E_ϕ) for a $\lambda/4$ monopole above the wings.

INSERT #1

1,2,2
4,0.,0.,18.81,1.,0.,0.25

INSERT #2

0.,0.
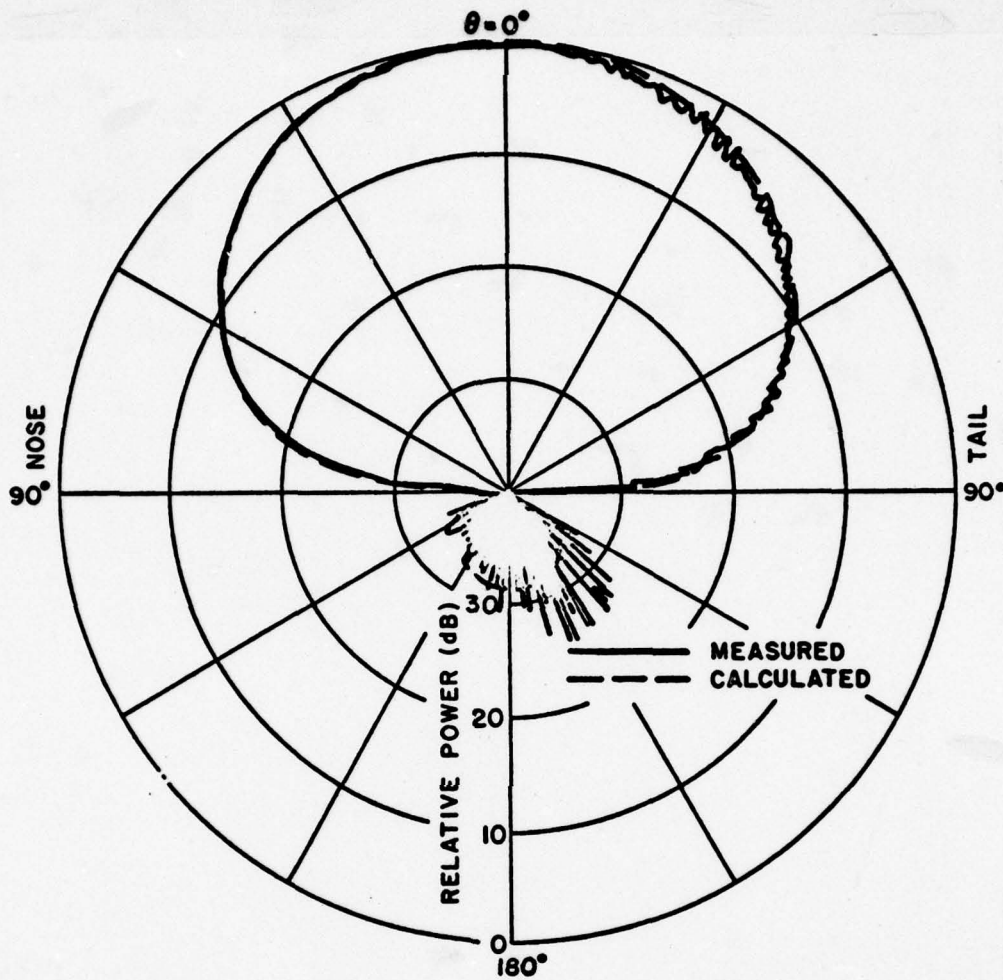
Figure 17a. Elevation plane pattern for an axial KA-band waveguide mounted forward of the wings on a KC-135 aircraft.

INSERT #1

3,2,2
2,0.,0.,8.34,1.,0.,.828
2,0.,.892,8.34,1.,0.,.828
2,0.,-.892,8.34,1.,0.,.828

INSERT #2

90.,-90.

44
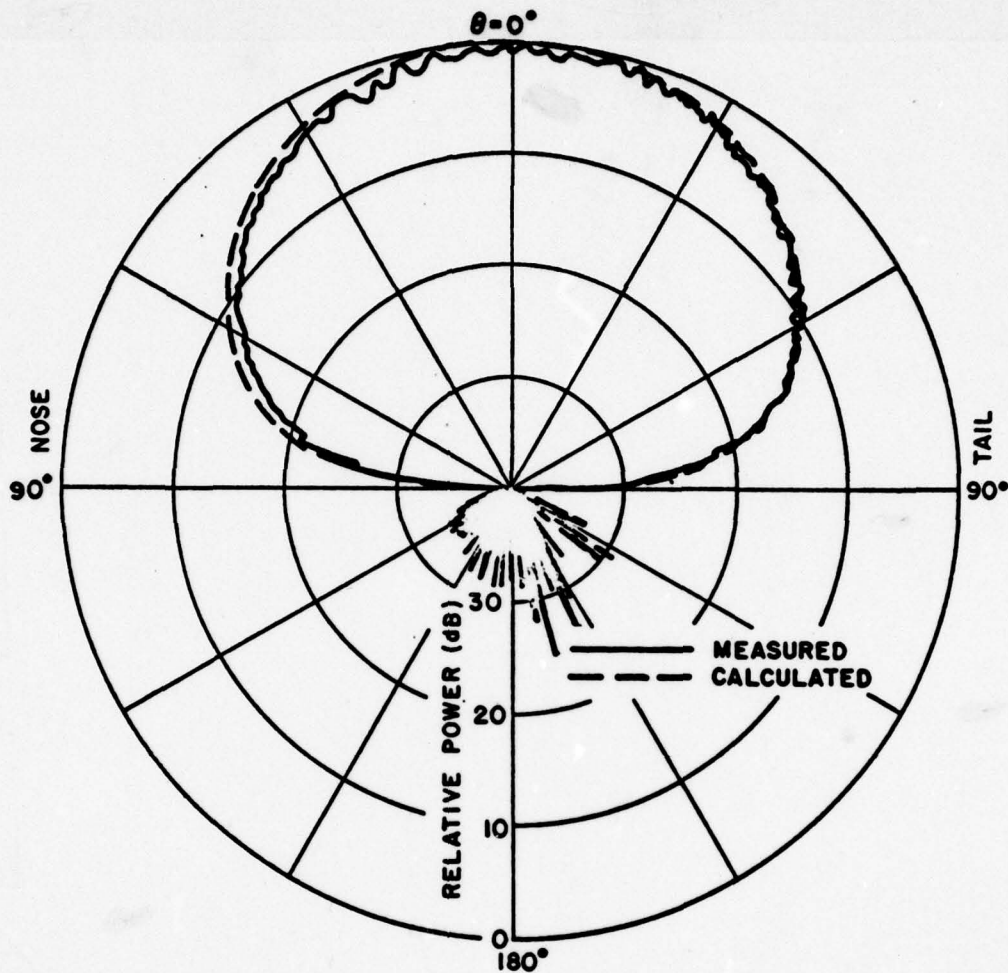
Figure 17b. Elevation plane pattern for an axial KA-band
waveguide mounted above the wings on a
KC-135 aircraft.

INSERT #1

3,2,2
2,0.,0.,18.81,1.,0.,.828
2,0.,0.892,18.81,1.,0.,.828
2,0.,-0.892,18.81,1.,0.,.828

INSERT #2

90.,-90.

45
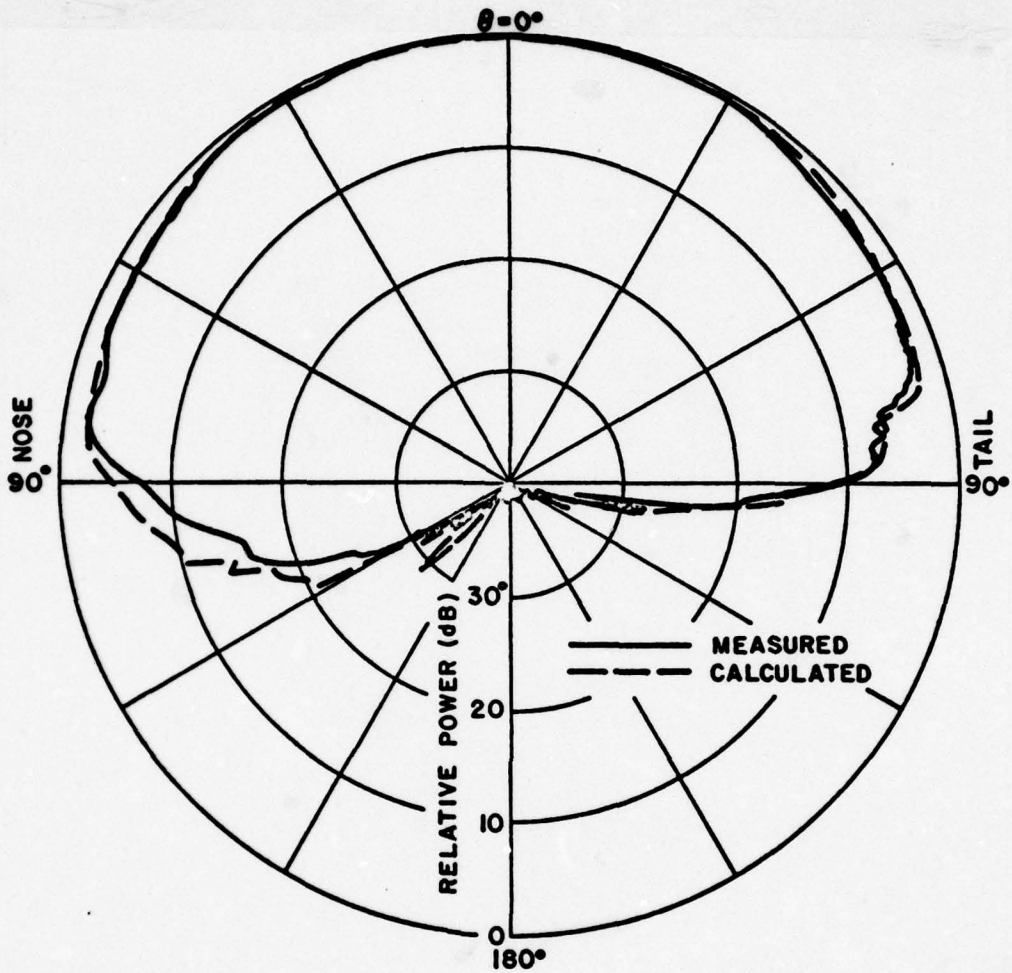
Figure 17c. Elevation plane pattern for a circumferential KA-band waveguide mounted forward of the wings on a KC-135 aircraft.

INSERT #1

3,2,2
2,90.,0.,8.2933,1.,0.,.828
2,90.,0.,8.34,1.,0.,.828
2,90.,0.,8.3867,1.,0.,.828

INSERT #2

90.,-90.

46
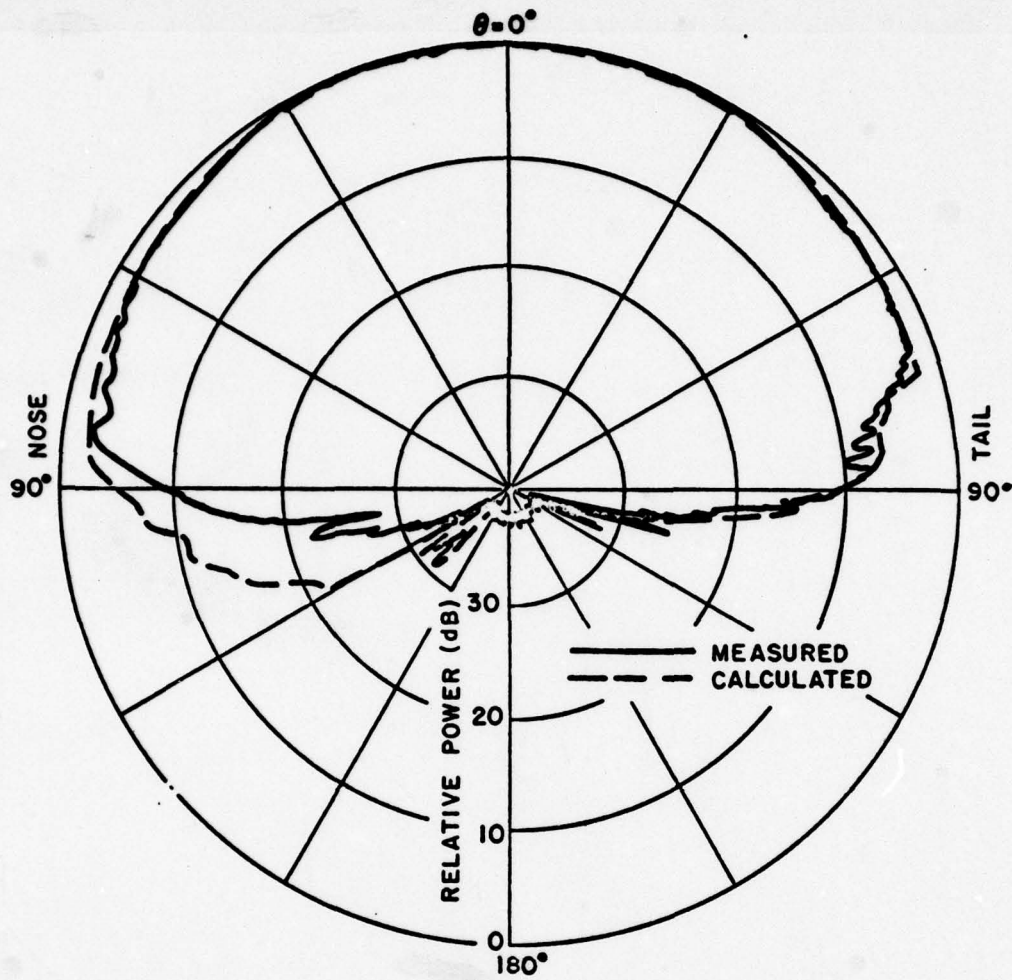
Figure 17d. Elevation plane pattern for a circumferential
KA-band waveguide mounted above the wings on
a KC-135 aircraft.

INSERT #1

3,2,2
2,90.,0.,18.7633,1.,0.,.828
2,90.,0.,18.81,1.,0.,.828
2,90.,0.,18.8567,1.,0.,.828

INSERT #2

90.,-90.

47
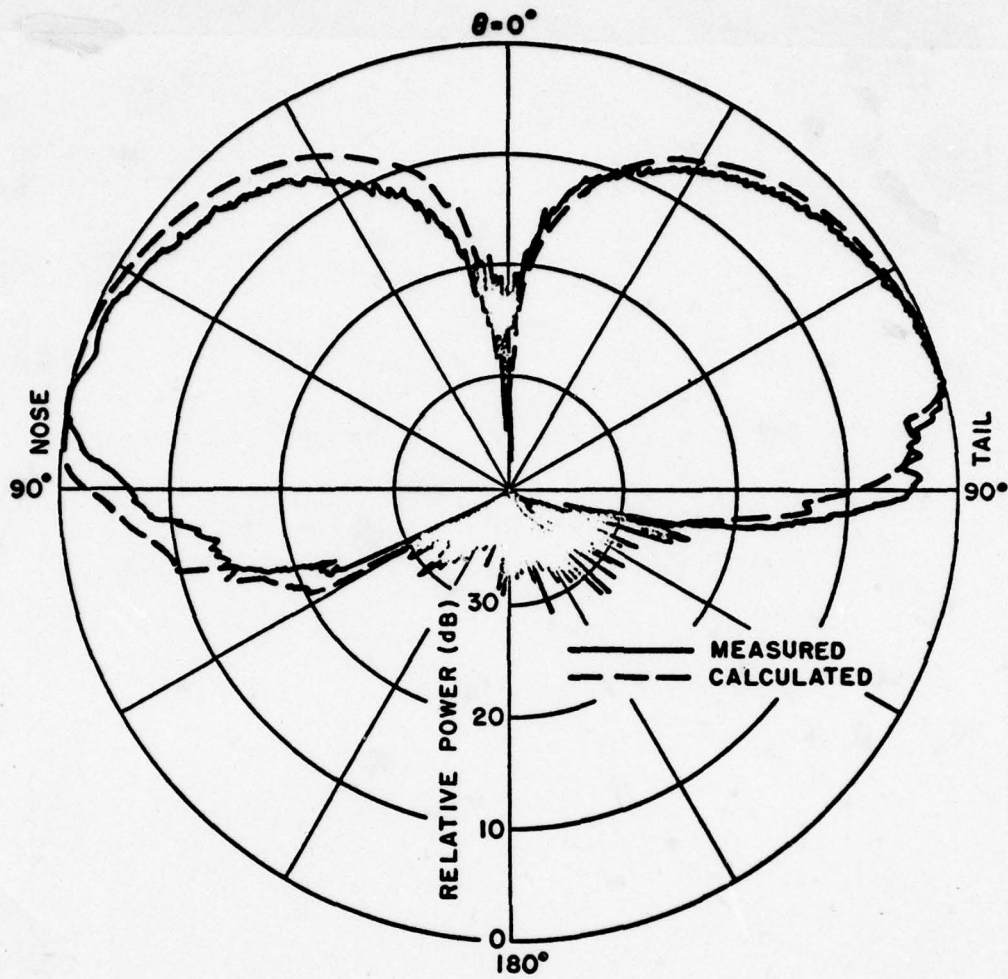
Figure 17e. Elevation plane pattern for a λ/4 monopole mounted
forward of the wings on a KC-135 aircraft.

INSERT #1   INSERT #2

1,2,2   90.,-90.
4,0.,0.,8.34,1.,0.,0.25

Figure 17f. Elevation plane pattern for a λ/4 monopole mounted above the wings on a KC-135 aircraft.

INSERT #1

1,2,2
4,0.,0.,18.81,1.,0.,0.25

INSERT #2

90.,-90.

3. Roll, elevation, and azimuth patterns are computed for a λ/4 monopole mounted at station 220 on a 737 aircraft as shown in Figure 13. The input data is given by:

```
T,F,F,F
65,86,43.3,43.3,58.72,308.56,1307.04,3.18
1,2,2
4,0.,0.,-278.,1.,0.,0.25
4,4
0.,43.3,56.54
0.,536.93,316.14
0.,536.93,379.86
0.,43.3,233.54
4,4,180.,T
0.,-43.3,233.54
0.,-536.93,379.86
0.,-536.93,316.14
0.,-43.3,56.54
4,4,180.,T
4,-6
0.,308.56,-31.585
-5.6,321.6,-27.07
-5.6,321.6,27.07
0.,308.56,31.585
4,4,180.,T
54.645,-478.4,0.
54.645,-613.76,8.25
284.147,-819.056,8.25
284.147,-683.696,0.
284.147,-819.056,-8.25
54.645,-613.76,-8.25
1,4,348.58,T
90,91,5,0,360,2  - - - - - - - - - - - - - - - - - - - - - - - }  INSERT
90,,0.  - - - - - - - - - - - - - - - - - - - - - - - - - - - - }
```

where the insert data is defined on each of the patterns as shown in Figure 18. Again the results are compared with measured patterns taken at NASA (Langley, Va.).
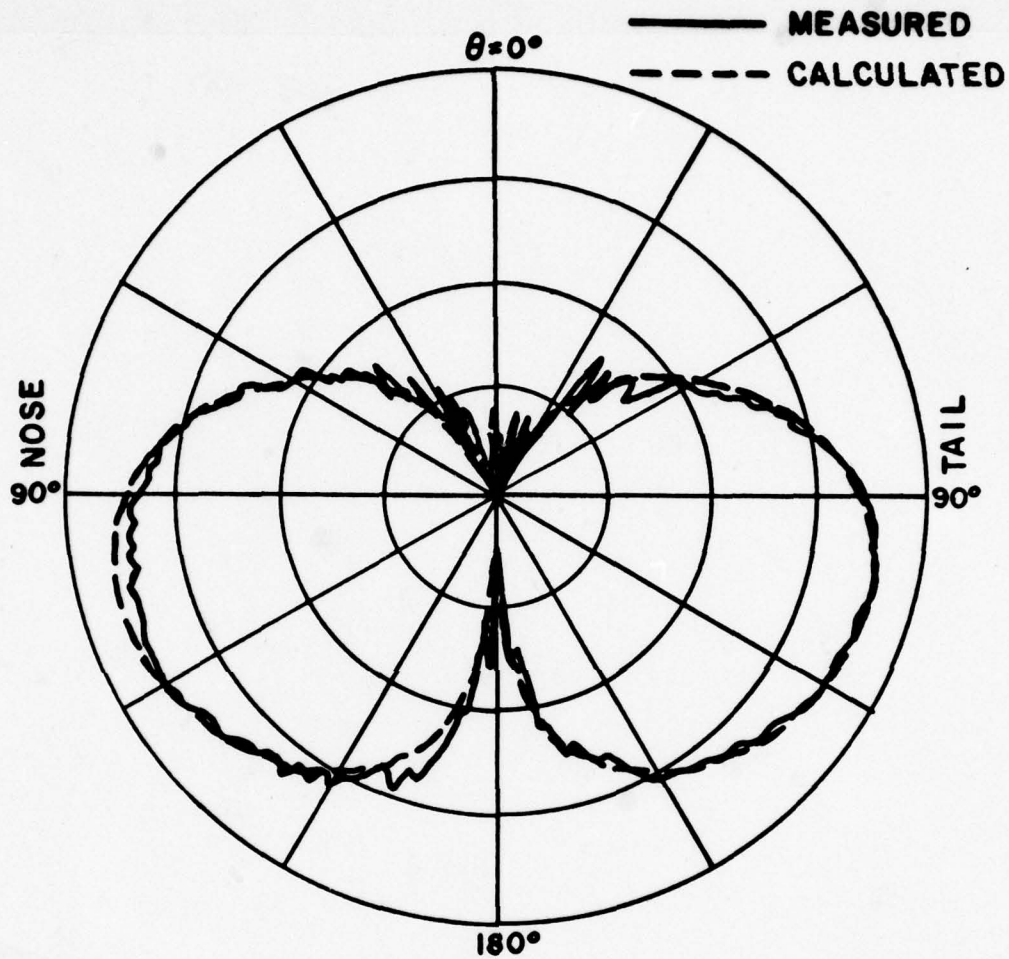
Figure 18a. Roll plane pattern of a λ/4 monopole mounted at
station 220 on top of a boeing 737 aircraft.
(φ = 90° at the left; φ = 270° at the right).

INSERT

0.,0.

51
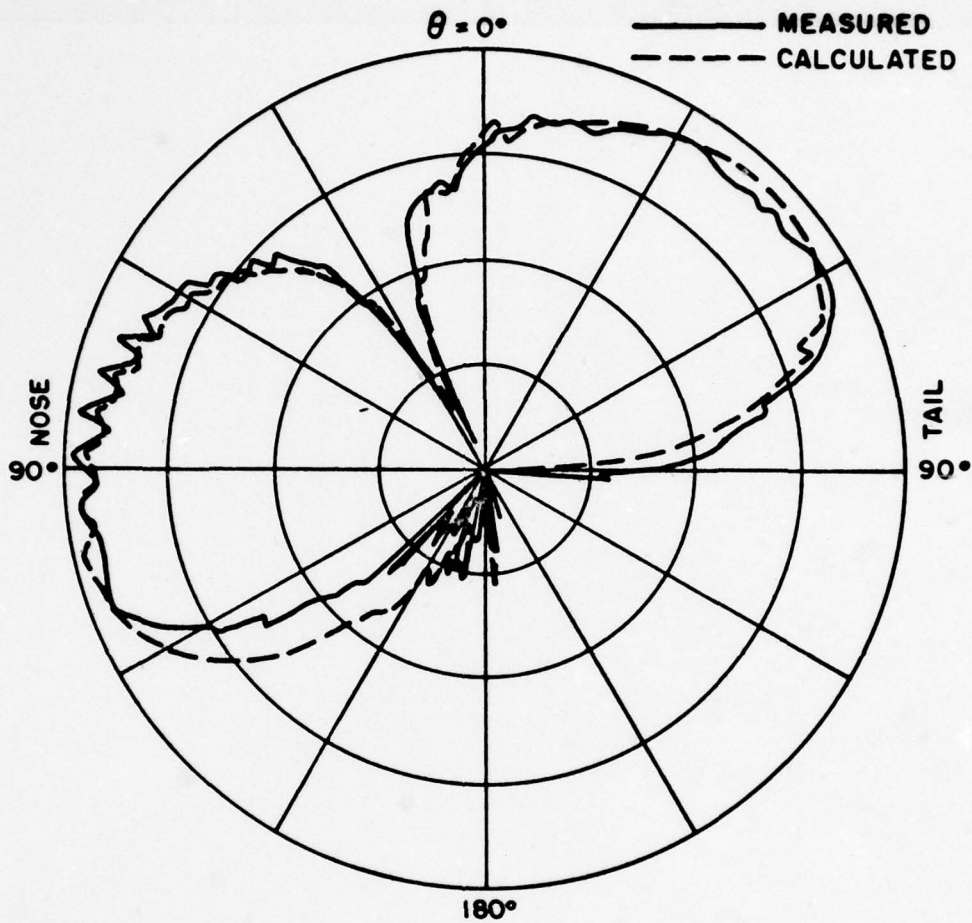
Figure 18b. Elevation plane pattern of a λ/4 monopole mounted
at station 220 on top of a Boeing 737 aircraft.
(φ = 0° at the left; φ = 180° at the right).

INSERT

90.,-90.

52
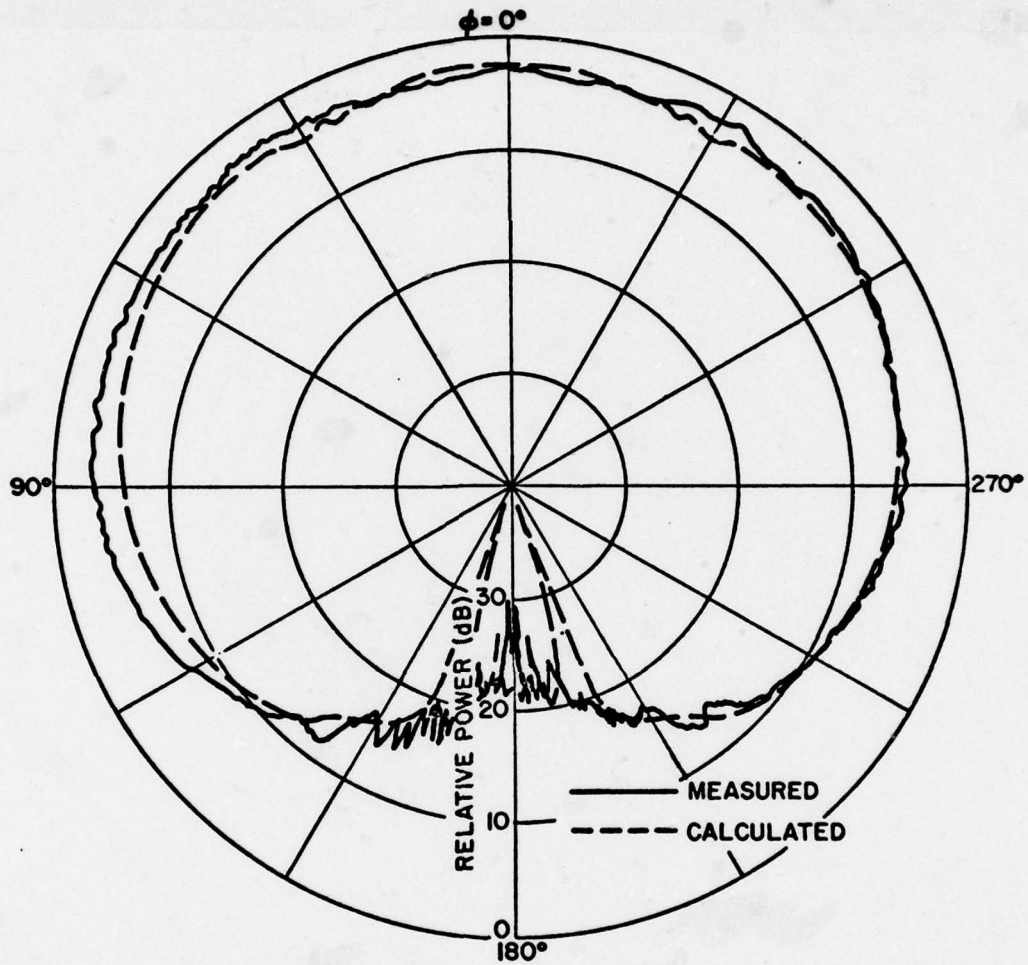
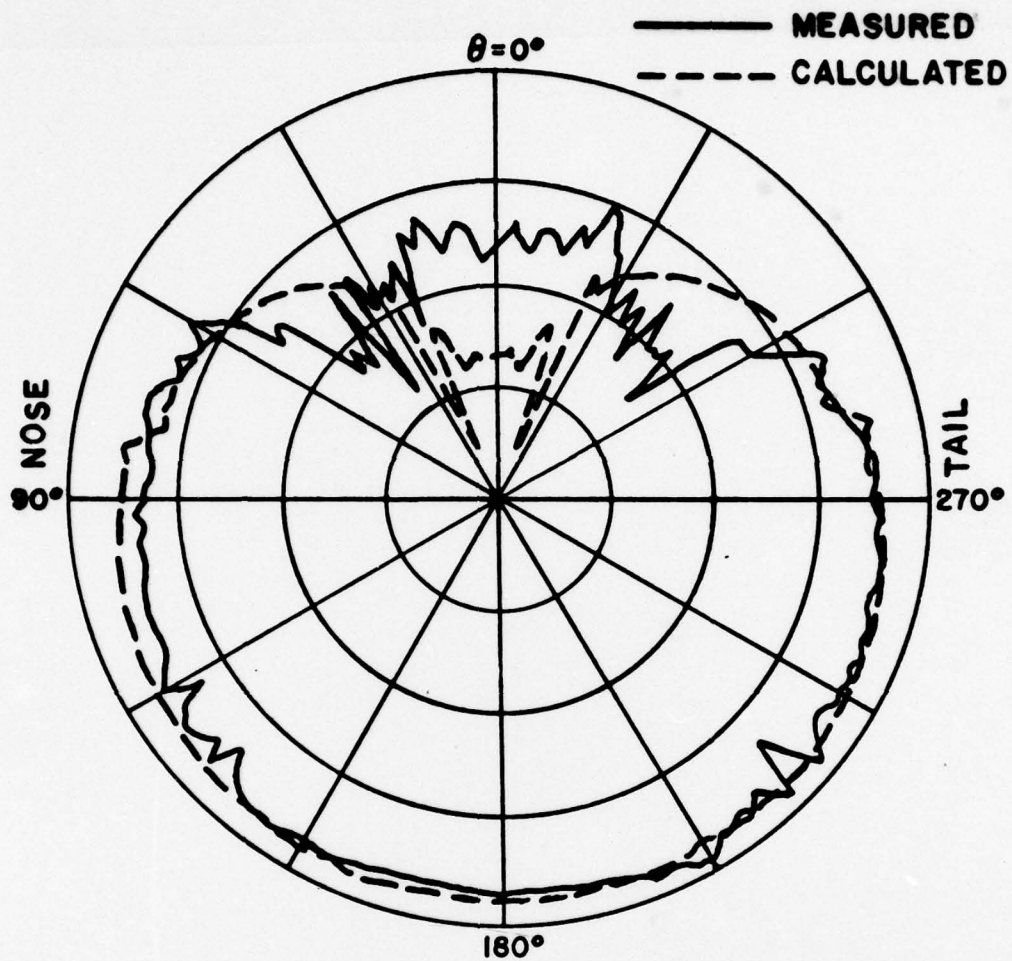Figure 18c. Azimuth plane pattern of a λ/4 monopole mounted at station 220 on top of a Boeing 737 aircraft.

INSERT

90.,0.

53

4. Roll, elevation, and azimuth patterns are computed for a λ/4
monopole mounted at station 950 on the belly of a 737 aircraft as shown in
Figure 19. The input is given by:

```
T,F,F,F
66.55,66.55,66.55,110.312,548.325,552.72,3.18
1,4,1
4,0.,0.,-270.72,1.,0.,0.25
4,4,4,4
-5.64,66.55,-544.824
-5.64,207.552,-591.072
-5.64,207.552,-532.416
-5.64,66.55,-413.976
4,4,180.,,T
-5.64,-66.55,-413.976
-5.64,-207.552,-532.416
-5.64,-207.552,-591.072
-5.64,66.55,-544.824
4,4,180.,,T
33.84,66.55,-31.58
33.84,529.03,-171.46
33.84,529.03,-110.54
33.84,66.55,137.62
4,4,180.,,T
33.84,-66.55,137.62
33.84,-529.03,-110.54
33.84,-529.03,-171.46
33.84,-66.55,-31.58
4,4,180.,,T
4
16.38,206.87,-38.
-4.51,257.184,-38.
-4.51,257.184,38.
16.38,206.87,38.
4,4,180.,,T
```

```
30,91,2,0,360,2  - - - - - - - - - - - - - - - - - ⎫
0.,0.            - - - - - - - - - - - - - - - - - - ⎬ INSERT
- - - - - - - - - - - - - - - - - - - - - - - - - - ⎭
```

where the insert data is defined on each of the patterns as shown in
Figure 20. The results are compared with measured patterns taken at
NASA (Langley, Va.). Note that in this case the antenna was actually
mounted on the belly of the aircraft; yet, the program requires the
model be turned over and computed as though the antenna were on top of
the aircraft.
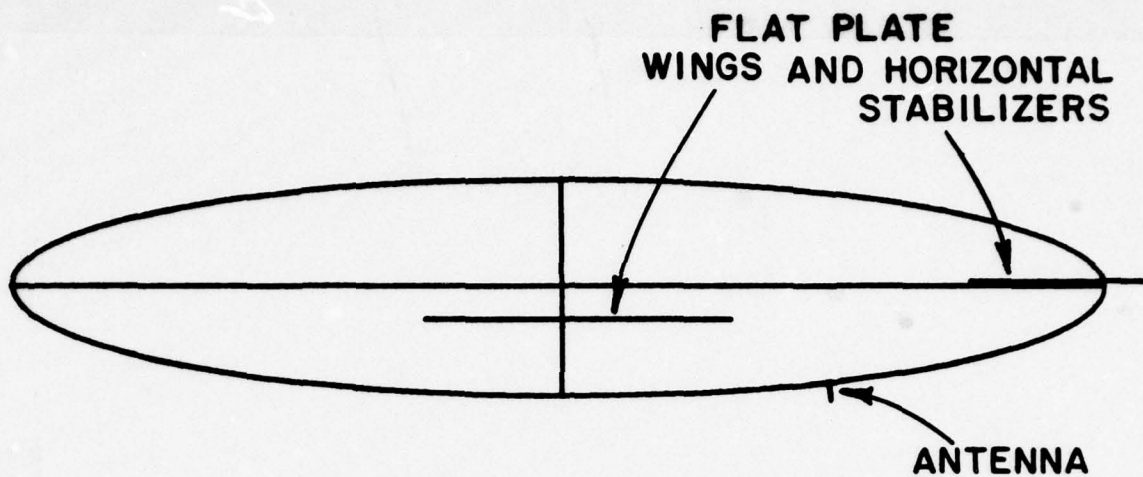
Figure 19a. Computer simulated model for the fuselage profile of a Boeing 737 aircraft (side view). The antenna is located at station 950 on the Bottom of the fuselage.
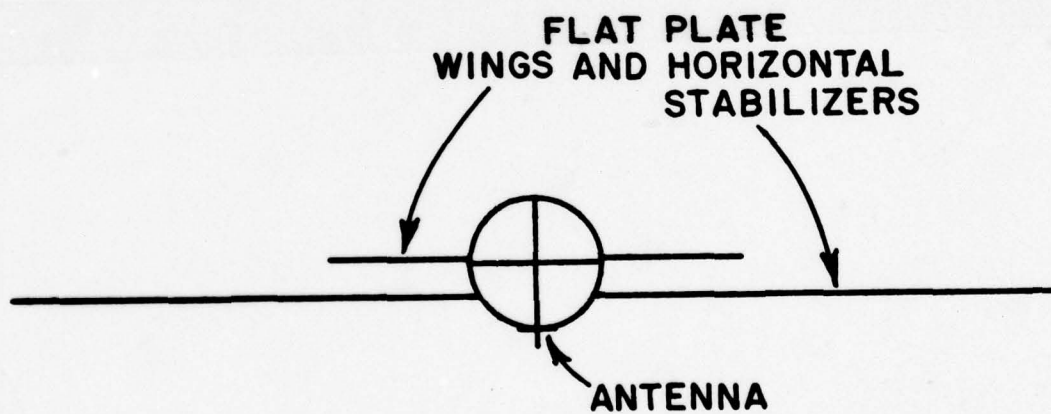
Figure 19b. Computer simulated model for the cross section (at antenna location) of a Boeing 737 aircraft (front view). The antenna is located at station 950 on the bottom of the fuselage.
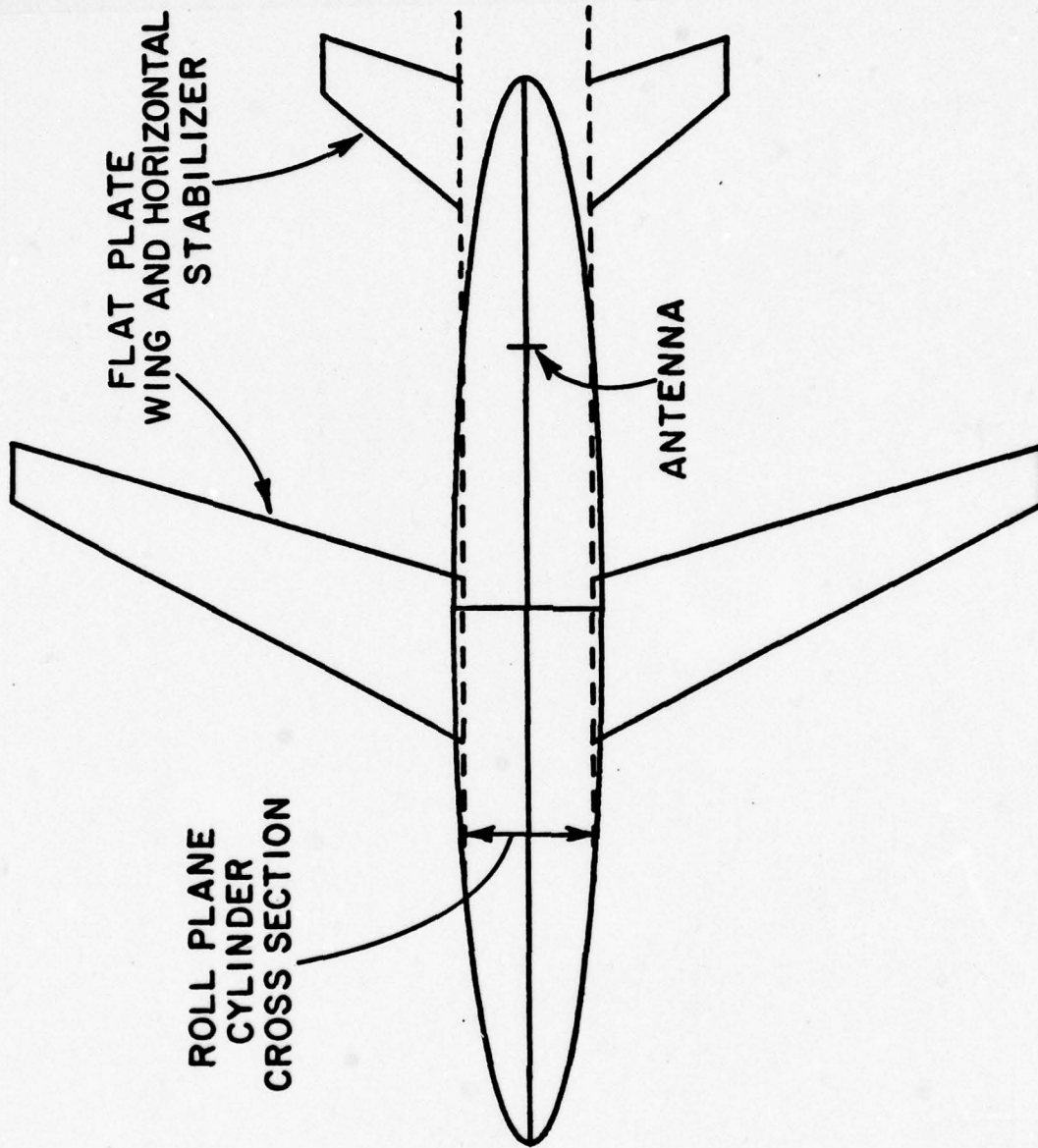
Figure 19c. Computer simulated model for a Boeing 737 aircraft (top view). The antenna is located at station 950 on the bottom of the fuselage.

56

Figure 20a. Roll plane pattern of a $\lambda/4$ monopole mounted at station 950 on the bottom of a Boeing 737 aircraft. ($\phi = 90°$ at the left; $\phi = 270°$ at the right).

INSERT

0.,0.
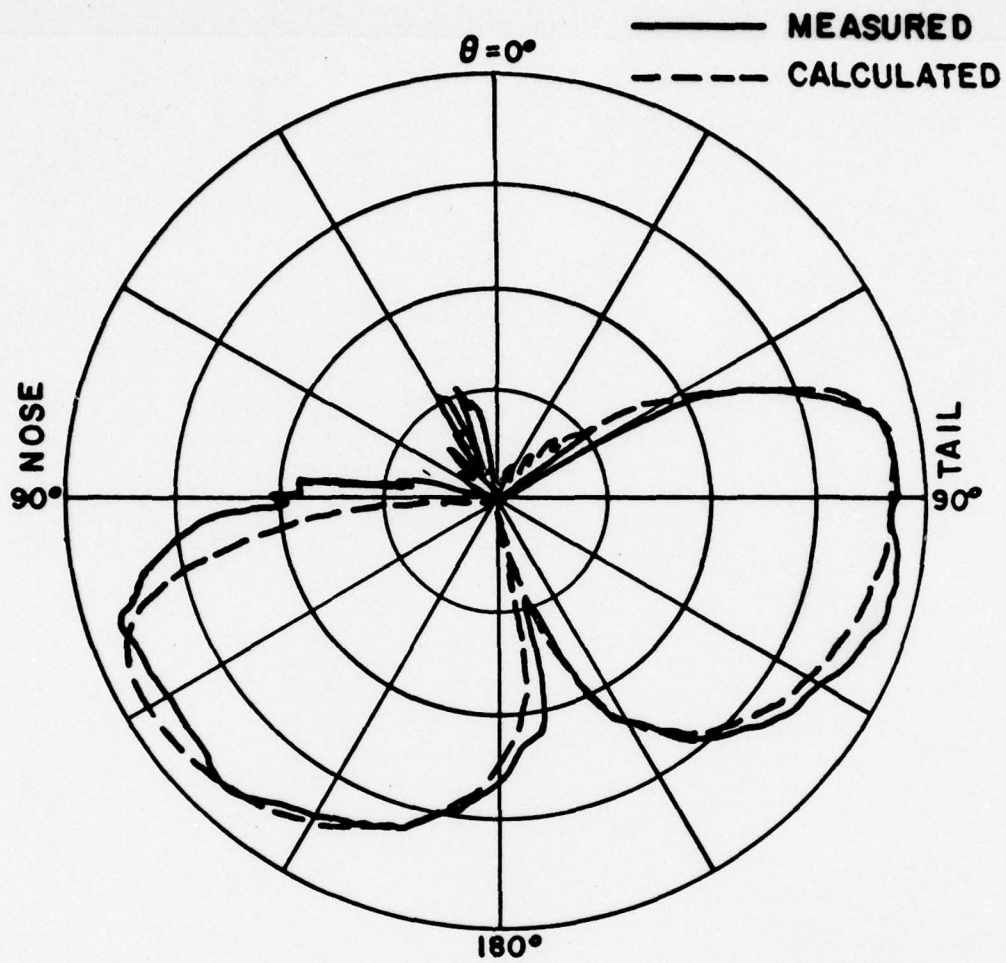
Figure 20b. Elevation plane pattern of a $\lambda/4$ monopole mounted at station 950 on the bottom of a Boeing 737 aircraft. ($\phi = 0°$ at the left; $\phi = 180°$ at the right).

INSERT

90.,-90.

Figure 20c. Azimuth plane pattern of a λ/4 monopole mounted at station 950 on the bottom of a Boeing 737 aircraft.

INSERT

90.,0.

5. Roll, elevation, and azimuth patterns are computed for a Lindberg crossed slot antenna mounted at station 470 on a KC-135 aircraft as shown in Figure 2[1]. The Lindberg crossed slot is a circularly polarized antenna and is described in Reference [9]. The input data for this geometry is given by:

```
T,F,F,F
3.,3.,3.,3.75,8.,80.,34.92
2,2,2
2,0.,0.,2.25,1.,0.,0.78
2,90.,0.,2.25,1.,90.,0.78
4,4
-1.,3.,12.31
-1.,28.5,36.41
-1.,28.5,40.41
-1.,3.,24.61
4,4,180.,T
-1.,-3.,24.61
-1.,-28.5,40.41
-1.,-28.5,36.41
-1.,-3.,12.31
4,4,180.,T
4,-6
1.5,7.35,-1.36039
.775,9.,-1.36039
.775,9.,1.36039
1.5,7.35,1.39039
4,4,180.,T
2.946,-49.492,0.
2.946,-55.672,0.5
14.076,-64.205,0.5
14.076,-58.025,0.
14.076,-64.205,-0.5
2.946,-55.672,-0.5
1,4,351.,T
90,91,5,0,360,2
0.,0.
```
} INSERT

where the insert data is given on each pattern as shown in Figure 22. The results can be compared with Lindberg's measured data [9] as shown in Figure 23. Note that the data is plotted as linear field components in that this data format was used by Lindberg. The E-theta and E-phi components can be combined to give

$$E_{CP} = \text{E-theta } e^{j90°} + \text{E-phi } e^{j0°},$$

where E_{CP} is the transmitted circularly polarized field. This data is plotted in Figure 24.

60
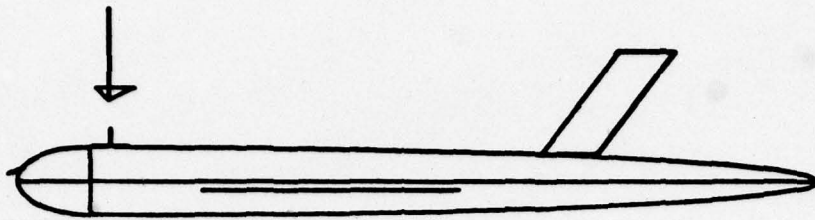
ANTENNA

Side view of computer model.
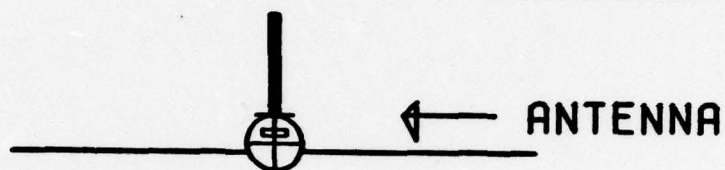
ANTENNA

Front view of computer model.
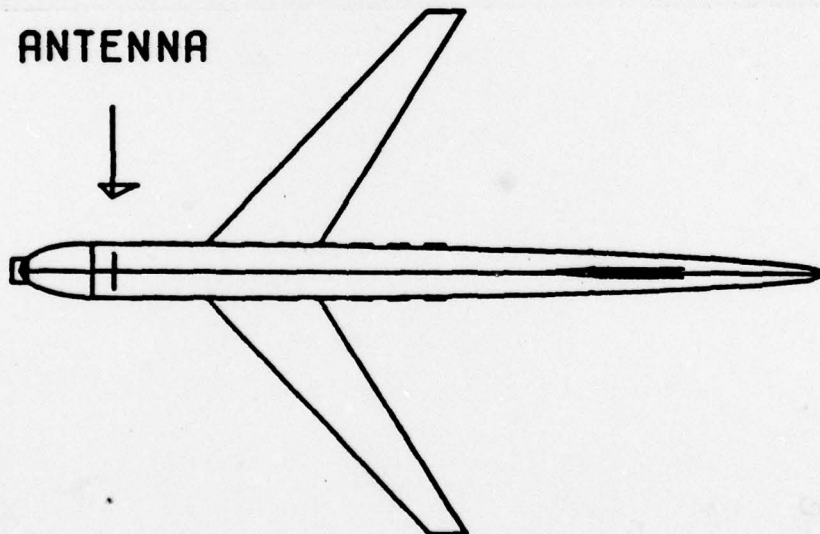
ANTENNA

Top view of computer model.

Figure 21.   Computer model used to simulate the KC-135 aircraft.
The Lindberg crossed slot location is identified at
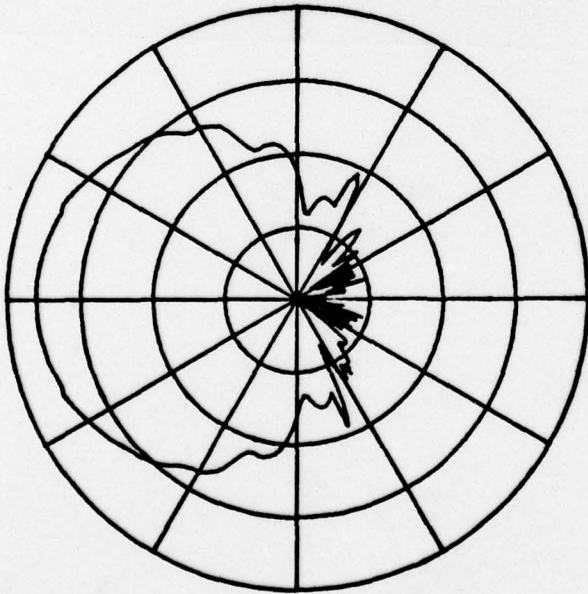station 470.

Figure 22b. Roll plane pattern (E_ϕ) of Lindberg crossed-slot antenna mounted at station 470 on KC-135 aircraft.
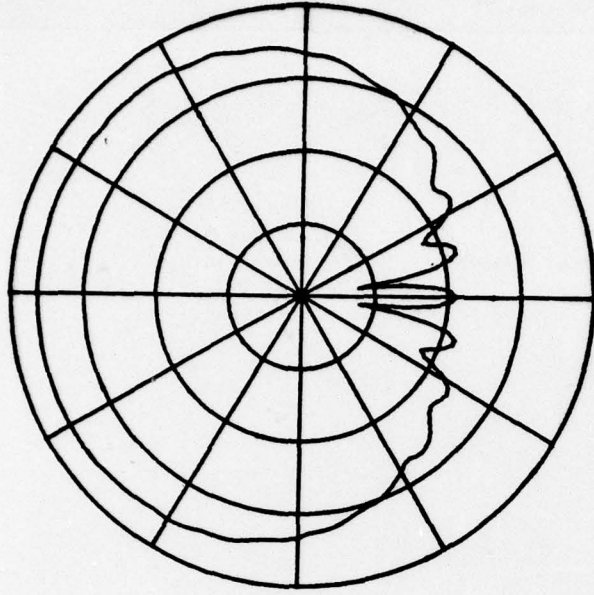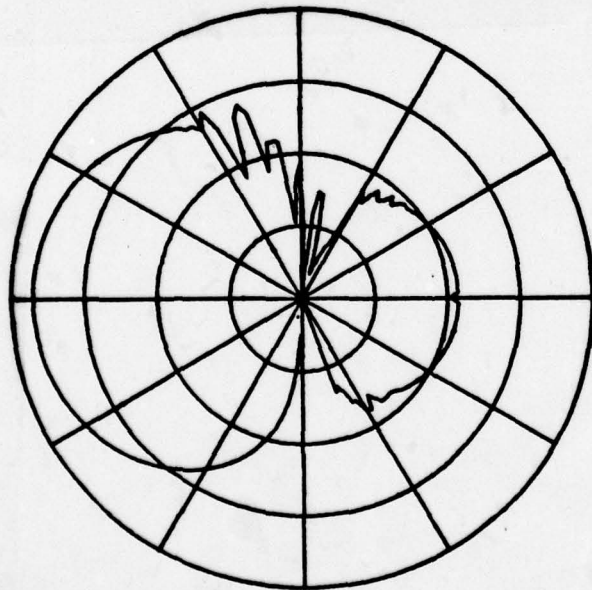
Figure 22a. Roll plane pattern (E_θ) of Lindberg crossed-slot antenna mounted at station 470 on a KC-135 aircraft.

Figure 22d. Elevation plane pattern (E_ϕ) of Lindberg crossed-slot antenna mounted at station 470 on a KC-135 aircraft.

INSERT
90.,-90.

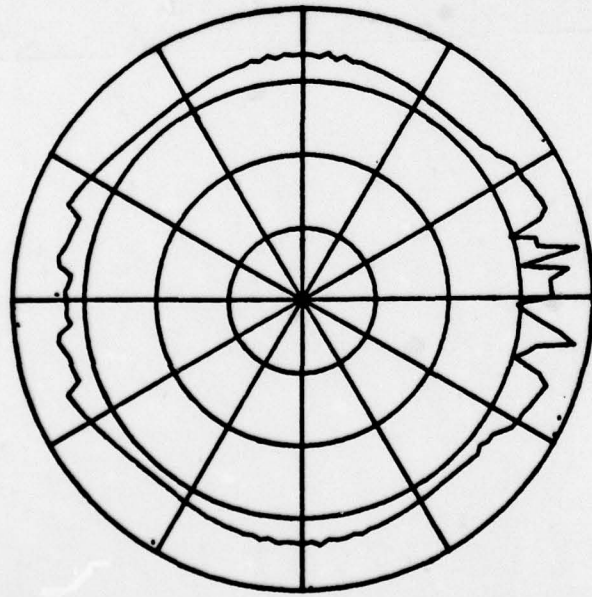Figure 22c. Elevation plane pattern (E_θ) of Lindberg crossed-slot antenna mounted at station 470 on a KC-135 aircraft.
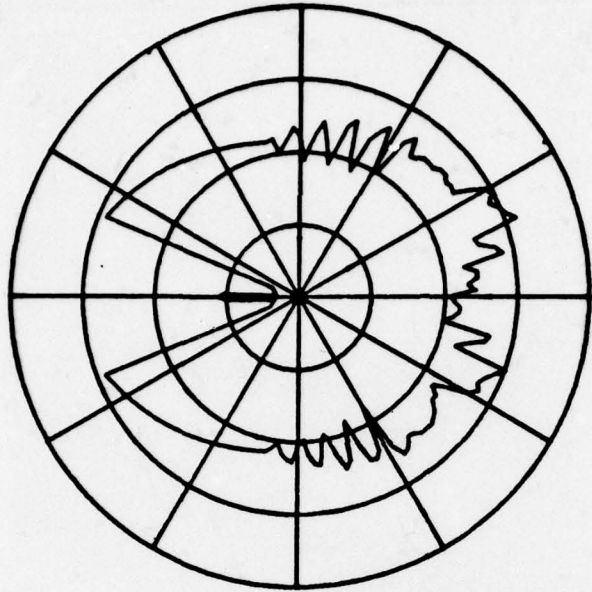
INSERT
90.,-90.

63

Figure 22f. Azimuth plane pattern (E_ϕ) of Lindberg crossed-slot antenna mounted at station 470 on a KC-135 aircraft.

INSERT
90.,0.

Figure 22e. Azimuth plane pattern (E_θ) of Lindberg crossed-slot antenna mounted at station 470 on a KC-135 aircraft.
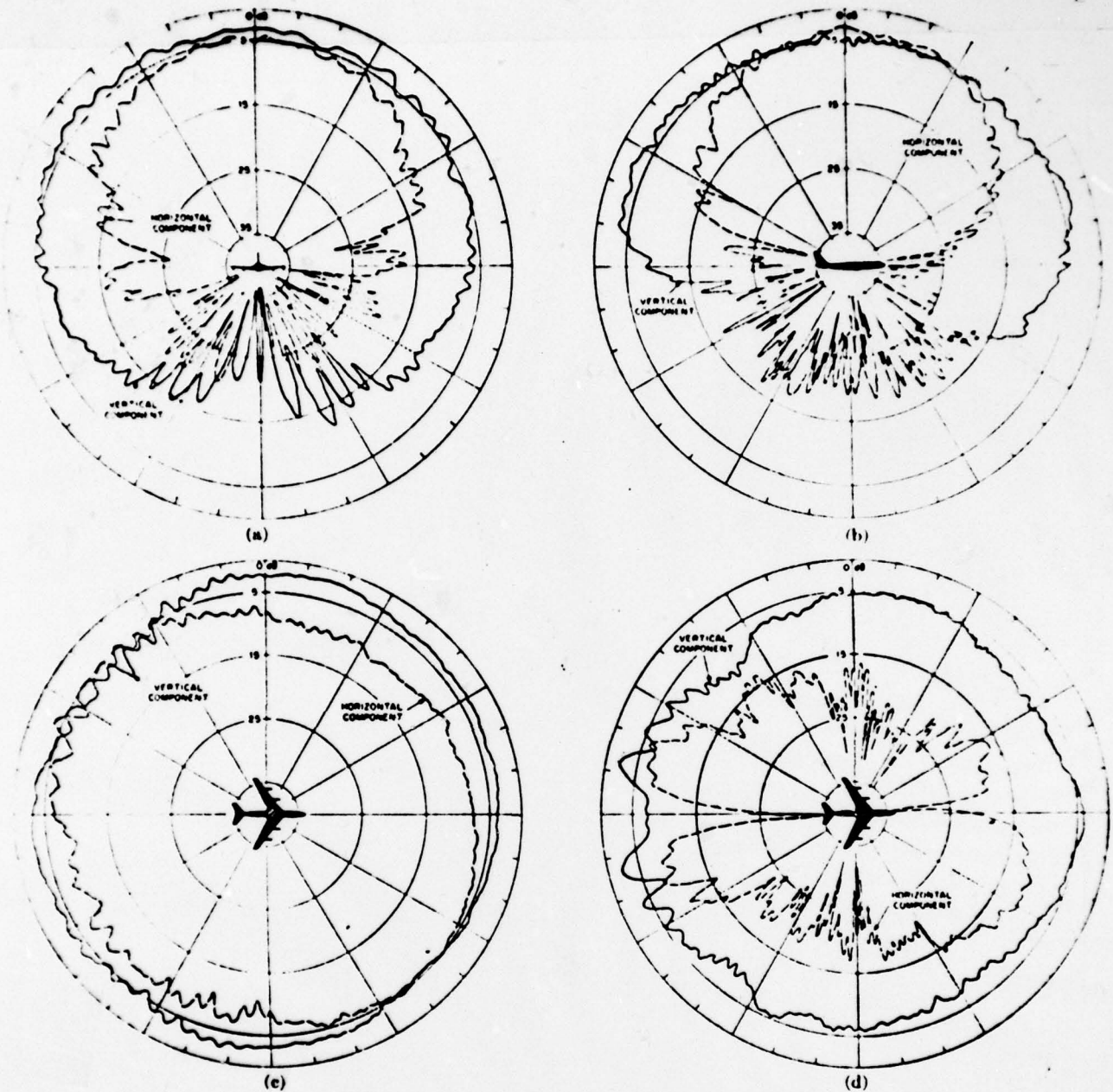
INSERT
90.,0.

Figure 23. Antenna radiation patterns, 1/25-scale-model measurements.
(a) Antenna location: station 470; slot length; 0.78λ;
transverse vertical. (b) Antenna location: station 470,
slot length; 0.78λ; longitudinal vertical. (c) Antenna
location: station 470; slot length; 0.78λ; conical cut
θ = 45 degrees. (d) Antenna location: station 470; slot
length; 0.78λ; horizontal plane. [Taken from Ref. 9]

65
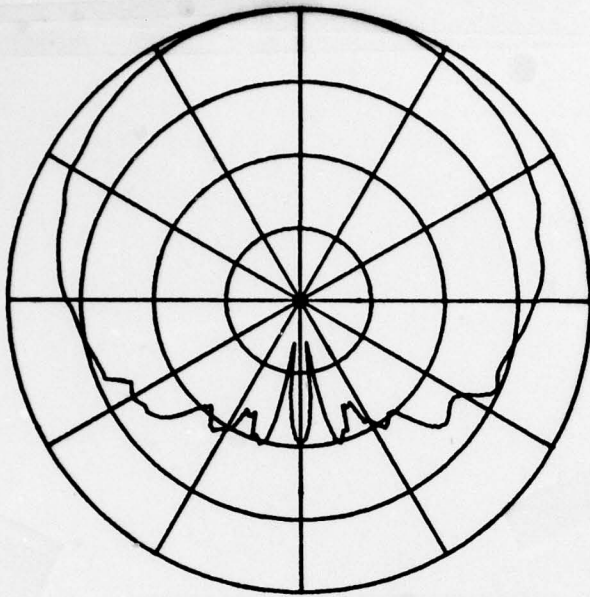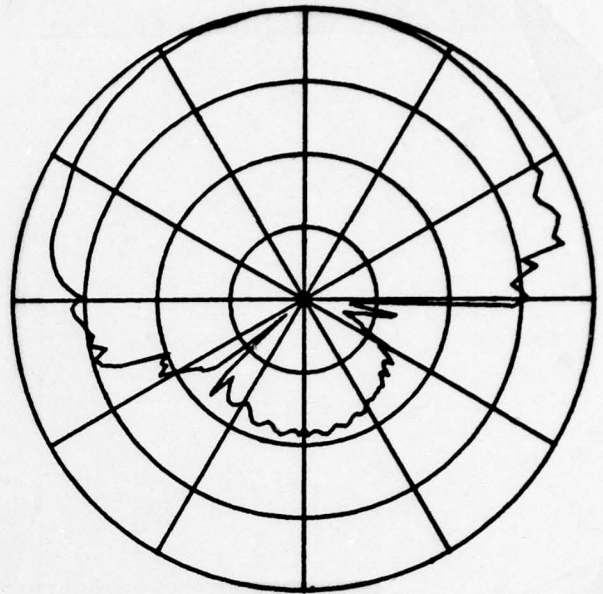
(a) roll pattern   (b) elevation pattern
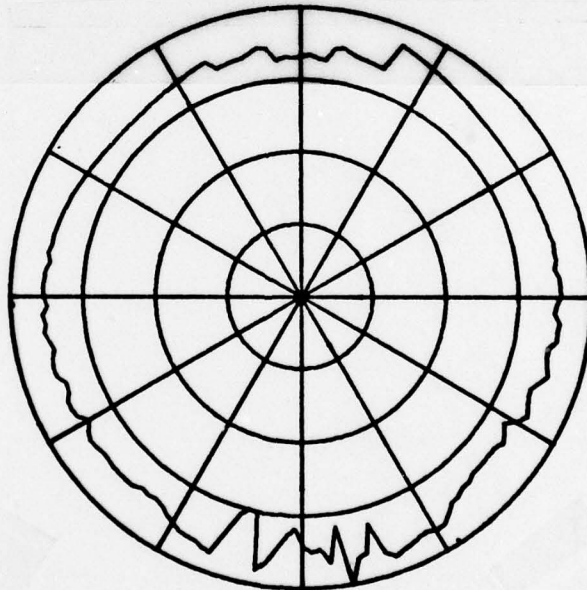
(c) azimuth pattern

Figure 24.   Pattern (E_{CP}) of Lindberg crossed-slot antenna mounted
at station 470 on a KC-135 aircraft.

66

VI. PROGRAM OUTPUT

The basic output from the computer code is a line printer listing of the results. Recall that the results of the program are the $E_\theta p$ and $E_\phi p$ radiation pattern values. In order to again describe these pattern components, let us consider the various principal plane patterns treated in the previous section. The computer code allows for a rotation of coordinates such that one can take a pattern about an arbitrary axis. This information is input to the code using the spherical angles THC, PHC. The geometry that applies for each of the roll, elevation, and azimuth patterns of previous section is illustrated in Figure 25. Note that the θp and ϕp angles are defined relative to the rotated pattern coordinates and that they change as THC, PHC is changed. Thus, $E_\theta p$ is the normal theta component of the field (i.e., $E_\theta p = \vec{E} \cdot \hat{\theta} p$). Likewise, $E_\phi p = \vec{E} \cdot \hat{\phi} p$. The total radiated electric field is denoted by $\vec{E}$.

In addition to the printed results, one has the option of obtaining a set of polar patterns. If LPLT=T in the input data list, the program will automatically plot the $E_\theta p$ and $E_\phi p$ polar patterns. These patterns are plotted such that the outer ring corresponds to the pattern maximum in each case. This polar plot routine was used to plot the data presented in the previous section.
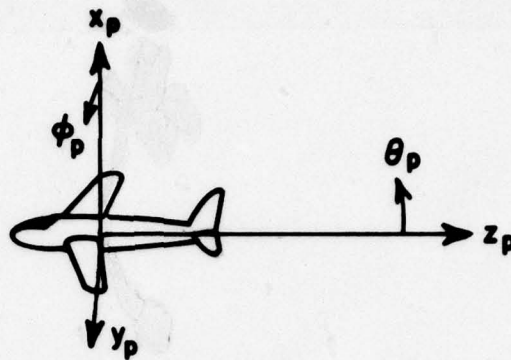
(a) ROLL PLANE COORDINATES
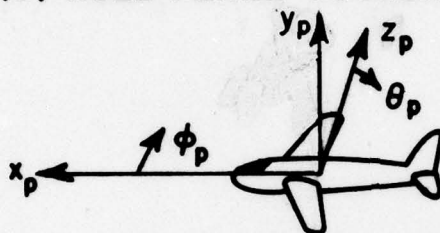
(b) ELEVATION PLANE COORDINATES
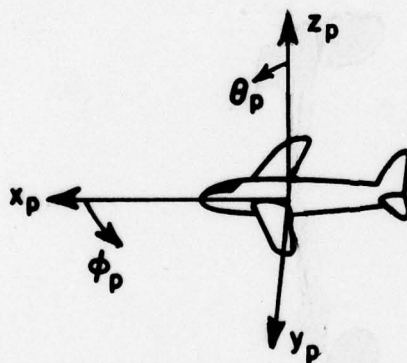
(c) AZIMUTH PLANE COORDINATES

Figure 25.   Illustration of pattern coordinates for the
principal plane pattern calculations.

68

REFERENCES

[1] W. D. Burnside, R. J. Marhefka and C. L. Yu, "Roll Plane Analysis of On-Aircraft Antennas," IEEE Trans. on Antennas and Propagation, Vol. AP-21, November 1973, pp. 780-786.

[2] W. D. Burnside, "Analysis of On-Aircraft Antenna Patterns," Report 3390-1, August 1972, The Ohio State University ElectroScience Laboratory, Department of Electrical Engineering; prepared under Contract N62269-72-C-0354 for Naval Air Development Center. (AD 777 989)

[3] R. J. Marhefka and W. D. Burnside, "Numerical Solutions to Some On-Aircraft Antenna Pattern Problems," Technical Report 3390-4, October 1973, The Ohio State University ElectroScience Laboratory, Department of Electrical Engineering; prepared under Contract N62269-72-C-0354 for Naval Air Development Center. (AD 777 977)

[4] W. D. Burnside, M. C. Gilreath, R. J. Marhefka and C. L. Yu, "A Study of KC-135 Aircraft Antenna Patterns," IEEE Trans. on Antennas and Propagation, Vol. AP-23, No. 3, May 1975, pp. 309-316.

[5] C. L. Yu and W. D. Burnside, "MLS Airborne Antenna Research," Semi-annual Report 2902-22, May 1975, The Ohio State University Electro-Science Laboratory, Department of Electrical Engineering; prepared under Grant NGL 36-003-138 for National Aeronautics and Space Administration, Langley Research Center.

[6] C. L. Yu and W. D. Burnside, "Research on MLS Airborne Antenna," Semi-Annual Report 2902-23, April 1976, The Ohio State University ElectroScience Laboratory, Department of Electrical Engineering; prepared under Grant NGL 36-003-138 for National Aeronautics and Space Administration, Langley Research Center.

[7] C. L. Yu and W. D. Burnside, "Volumetric Pattern Analysis of Fuselage-Mounted Airborne Antennas," Report 2902-24, April 1976, The Ohio State University ElectroScience Laboratory, Department of Electrical Engineering; prepared under Grant NGL 36-008-138 for National Aeronautics and Space Administration, Washington, D.C.

[8] R. M. Janes, All the World's Aircraft, 1973-1974, McGraw-Hill Co.

[9] C. A. Lindberg, "A Shallow-Cavity UHF Crossed-Slot Antenna," IEEE Trans. AP-17, September 1969, pp. 558-563.

APPENDIX A - BEST-FIT ELLIPSE ANALYSIS

The elliptic cylinders necessary to simulate the fuselage profile and cross-section can be found using a best fit routine through the use of a digital computer. A best fit ellipse or composite ellipse is generated through a numerical process by inputting data points that described the surface of the profile or cross-section of the actual aircraft fuselage. Before these data points can be generated, a reference Cartesian coordinates system is needed on a scale model drawing of the aircraft. These coordinates can be best located by aligning one of the axes with the center line of the aircraft fuselage with the origin being arbitrarily chosen according to convenience. After the coordinate system is fixed, the position of data points on the profile or cross-section is measured from the scale model relative to the reference origin. The data points are taken in such a way that more points are specified around the antenna location and less points away from the source. This is due to the fact that the surface profile is dominant near the antenna location as described earlier. Figure 26 illustrates the way data points are taken from the fuselage profile. By feeding these data points into the best fit routine and adjusting the origin of the coordinates in the routine, an ellipse is found to best fit these data points.

The theory behind the best fit routine is that a function is to be found which best approximates a set of points in a least mean square error sense. For our computer model, a best fit ellipse is desired. The mathematical expression for an ellipse is

$$\frac{x^2}{a^2} + \frac{y^2}{b^2} = 1 \tag{A-1}$$

with its origin located at point (x=0, y=0). The parameters a and b are the semi-major and minor axes of an ellipse. To simplify the mathematical expression, Equation (A-1) can be written as

$$AX + BY = 1 \tag{A-2}$$

where $X = x^2$, $Y = y^2$, $A = \frac{1}{a^2}$, and $B = \frac{1}{b^2}$. Let (x_i, y_i), $i = 1, \cdots n$,

be n points from which a best fit ellipse is to be generated. Substituting these points into Equation (A-2), one obtains a set of n linear equations.

70
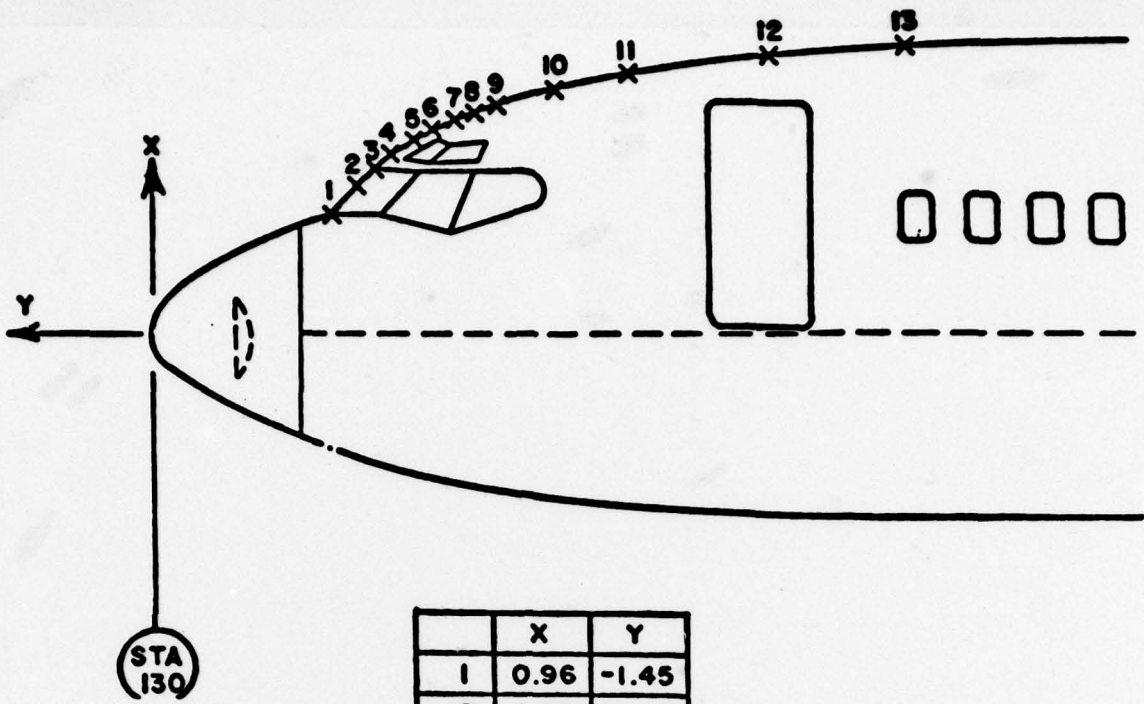
	X	Y
1	0.96	-1.45
2	1.20	-1.69
3	1.34	-1.82
4	1.45	-1.98
5	1.56	-2.16
6*	1.64	-2.30
7	1.69	-2.45
8	1.77	-2.60
9	1.84	-2.80
10	1.98	-3.28
11	2.08	-3.90
12	2.23	-5.01
13	2.30	-6.16
14	2.42	-10.14
15	2.44	-15.72
16	2.28	-24.10

* Antenna Location

Figure 26. Illustration of data points taken from the scale model aircraft for the determination of best fit elliptic cylinder using a digital computer.

71

$$AX_1 + BY_1 = 1$$

$$AX_2 + BY_2 = 1$$

$$\vdots \qquad \vdots \qquad \vdots$$

$$AX_n + BY_n = 1.$$

In matrix form, these n equations become

$$ZC = I, \text{ where } \quad Z = \begin{bmatrix} X_1 & Y_1 \\ X_2 & Y_2 \\ \cdot & \cdot \\ \cdot & \cdot \\ \cdot & \cdot \\ X_n & Y_n \end{bmatrix} \quad C = \begin{bmatrix} A \\ B \end{bmatrix} \text{ and } \quad I = \begin{bmatrix} 1 \\ 1 \\ \cdot \\ \cdot \\ \cdot \\ 1 \end{bmatrix} \tag{A-3}$$

By multiplying both sides of Equation (A-3) by $\tilde{Z}$, the transposed of Z, one obtains a simple 2x2 matrix as given by

$$\tilde{Z} \, ZC = \tilde{Z} \, I$$

$$\begin{bmatrix} \sum\limits_{m=1}^{n} X_m^2 & \sum\limits_{m=1}^{n} X_m Y_m \\ & \\ \sum\limits_{m=1}^{n} X_m Y_m & \sum\limits_{m=1}^{n} Y_m^2 \end{bmatrix} \begin{bmatrix} A \\ \\ B \end{bmatrix} = \begin{bmatrix} \sum\limits_{m=1}^{n} X_m \\ \\ \sum\limits_{m=1}^{n} Y_m \end{bmatrix} \tag{A-4}$$

which can be simply solved for A and B in the least mean square error sense. Thus, the ellipse parameters are defined.

The above approach works fine provided the origin of the ellipse is known in that Equation (A-1) assumes that x=y=0 is the origin. Consequently, one must specify an origin, then specify the "n" data points $[(x_i, y_i),\ 1 \le i \le n]$ relative to the chosen origin. One then solves Equation (A-4) and obtains the values for the ellipse (A and B). This elliptic curve is compared with the actual data and an error criterion developed. Thus, the procedure is to move the origin, obtain A and B, check the error, and proceed until the error is minimized. This is not difficult in that the origin of the elliptic curve is rather easily identified from the scale model drawings.

72